의학박사 학위논문

Comprehensive gene expression analyses of immunohistochemically defined subgroups of muscle-invasive urinary bladder urothelial carcinoma

면역조직화학염색을 통해 분류한 근육침윤성 방광 요로상피암 소집단간의 분자유전학적 발현 비교 분석

2021년 8월

서울대학교 대학원
의학과 병리학 전공

김 보 현

면역조직화학염색을 통해 분류한 근육침윤성 방광 요로상피암 소집단간의 분자유전학적 발현 비교 분석

지도교수 문 경 철

이 논문을 의학박사 학위논문으로 제출함
2021년 4월

서울대학교 대학원
의학과 병리학 전공
김 보 현

김보현의 의학박사 학위논문을 인준함
2021년 7월

위 원 장 _____

부위원장 _____

위 원 _____

위 원 _____

위 원 _____

Abstract

Comprehensive gene expression analyses of immunohistochemically defined subgroups of muscle-invasive urinary bladder urothelial carcinoma

Bohyun Kim
Department of Pathology
The Graduate School
Seoul National University

Introduction: A number of urinary bladder urothelial carcinoma (UBUC) mRNA-based classification systems have been reported. It also has been observed that treatment response and prognosis are different for each molecular subtype.

Material and methods: In this study, cytokeratin (CK)5/6 and CK20 immunohistochemistry (IHC) were performed, and IHC-based subgroup classification was applied. UB UC was classified into CK5/6 single-positive (SP), CK20 SP, double-positive (DP) and double-negative (DN) subgroups, and transcriptional analysis was performed. In addition, IHC staining for CK5/6, CK20, CK14, CD44, GATA3, FOXA1 and programmed cell death-ligand 1 (PD-L1) was performed on 189 muscle-invasive urinary bladder urothelial carcinoma (MIBC) using tissue microarray.

Results: The results of gene ontology terms and functional analysis

using differentially expressed genes indicate that, CK5/6 SP and DP subgroups were enriched in cell migration, immune activation, IL6-JAK-STAT3 signaling pathway and tumor necrosis factor-α signaling via nuclear factor-κB signaling pathway signature gene. In addition, compared with the other subgroups, the DN subgroup showed inhibited cell movement, cell migration, and cell activation. We evaluated PD-L1 expression by the SP142, SP263 and 22C3 assays, and classified the cases "positive" or "negative" according to the manufacturer's recommendations. The high positivity in the SP142, SP263 and 22C3 assay were significantly correlated with positive CK5/6, CK14 and CD44 expression, negative CK20, GATA3 and FOXA1 expression. The CK5/6 SP subgroup showed high positivity in the SP142, SP263 and 22C3 assay. Furthermore, in survival analysis, the CK5/6 SP subgroup was significantly associated with poor progression-free survival (p = 0.008).

Conclusions: These results suggests that the IHC-defined subgroups may be important to apply the PD-1/PD-L1 blockades in MIBC. And our study indicates that the CK5/6-positive group exhibited high gene expression signature related to aggressive behavior and exhibited worse clinical outcome.

Keyword: muscle invasive bladder cancer; molecular classification; immunohistochemistry; cytokeratin 5/6; cytokeratin 20; PD-L1

Student Number: 2015-31203

Table of Contents

List of Tables

List of Figures

List of Abbreviations

AJCC	American Joint Committee on Cancer
BASQ	Basal-squamous-like
CK	Cytokeratin
CK20 SP	Cytokeratin 20 single-positive
CK5/6 SP	Cytokeratin 5/6 single-positive
CPS	Combined positive score
DEGs	Differential expression genes
DN	Double-negative
DP	Double-positive
EMT	Epithelial-mesenchymal transition
FFPE	Formalin-fixed paraffin-embedded
GO	Gene ontology
GSEA	Gene set enrichment analysis
HPF	High power field
IC	Immune cells
IC+	Percentage of tumor-associated immune cells with staining
ICP	Immune cells present (percent of tumor area occupied by any tumor-associated immune cells)
IHC	Immunohistochemistry
IPA	Ingenuity Pathway Analysis

IRB	Institutional Review Board
KEGG	Kyoto Encyclopedia of Genes and Genomes
MIBC	Muscle-invasive urinary bladder cancer
MAPK	Mitogen-activated protein kinase
MiR	MicroRNA
NF-κB	Nuclear factor-κB
NGS	Next-generation sequencing
OS	Overall survival
PD-1	Programmed cell death-1
PD-L1	Programmed cell death-ligand 1
PFS	Progression-free survival
SNUH	Seoul National University Hospital
SP	Single-positive
TC	Tumor cells
TMA	Tissue microarray
TNF	Tumor necrosis factor
UB UC	Urinary bladder urothelial carcinoma
UC	Urothelial carcinoma
WHO/ISUP	World Health Organization/ International Society of Urologic Pathologists

1. Introduction

Bladder cancer is worldwide the 10th most common form of malignant tumor, and has the 14th highest cancer associated mortality [1]. Urinary bladder urothelial carcinoma (UB UC) is the most common tumor found in the urinary bladder. UB UC can be divided into papillary urothelial carcinoma (UC), which shows papillary growth, and invasive UC, which initially shows invasive growth. The two type tumors are known to have different pathogenesis. Recent studies reported that papillary UC originate from the intermediate cells of the urothelium, and that carcinoma in situ and invasive UC originate from the basal cells of the urothelium [2].

Recently, several studies have been published, which utilized next-generation sequencing (NGS) analysis to analyze and classify UB UC according to gene expression [3-5]. While several different mRNA-based subtype classifications exist, some of them overlap with one another. Universally, UB UC is classified into luminal and basal subtypes, and according to each classification system it is further classified into TP53-like type, urothelial-like A type, infiltrated type, genomically unstable type, mesenchymal-like type, and small cell/neuroendocrine-like type [3]. Each subtype shows high expression of specific genes. While the basal type shows high expression of stem cell or basal urothelial cell markers such as *KRT14, KRT5, KRT6*, and *CD44*, the luminal type shows high expression of urothelial differentiation markers such as *KRT20, GATA3,* and *FOXA1* [3, 5]. Furthermore, consistent with gene expression in each subtype, on immunohistochemistry (IHC) staining, the basal type shows high expression of cytokeratin (CK)5/6, and the luminal type shows high expression of CK20 [3, 5]. Through the consensus meeting, bladder cancers showing positive *KRT5/6, KRT14* expression and negative *GATA3, FOXA1* expression were classified into a specific subtype called Basal-Squamous-like (BASQ) [6]. In one study, the BASQ group was

reported to show a tumor phenotype with high KRT6 and KRT14 and low FOXA1 and GATA3 expression by IHC [7].

Molecular subtypes for UB UC have been established recently, and studies attempting to demonstrate their clinical significance are actively in progress [8]. Molecular subtype classification in UB UC also has the potential to play a major role in treatment decision and prognosis prediction [9, 10]. In fact, various studies have reported that prognosis, neoadjuvant chemotherapy response, and targeted therapy gene mutation vary among molecular subtypes in UB UC. Neoadjuvant cisplatin-based chemotherapy is the standard of care for high-risk muscle-invasive urinary bladder UC (MIBC). Neoadjuvant chemotherapy response varies among with molecular subtype, especially the TP53-like subtype, which is known to be chemo-resistant, and basal-type MIBC, which is reported to benefit from neoadjuvant chemotherapy because of its chemo-sensitive nature [3, 11].

In a phase II clinical trial of IMvigor210, different treatment responses to the immune check point inhibitor atezolizumab and prognosis were reported among molecular subtypes in patients with locally advanced UC. In phase II clinical trial of CheckMate 275 using nivolumab, another immune check point inhibitor, different treatment responses were reported among molecular subtypes in patients with advanced stage UC [12-15]. In addition, Hodgson et al. suggested distinguishing luminal and basal subtypes of MIBC using CK 5/6 and GATA3 IHC, and after such classification, the basal subtype showed a significant association with the abundance of CD8+ T cell expression and with high programmed cell death-ligand 1 (PD-L1) positivity identified by the SP263 assay [16].

HER2 overexpression and *ERBB2* gene amplification is known to be common in breast cancer, stomach cancer, and also in MIBC. Recently, HER2 protein overexpression and gene amplification have been reported in UC, and some studies have shown the prognostic significance of HER2 overexpression or gene amplification in UC [17-20]. The frequency of HER2 overexpression or gene

amplification in UC is approximately 10% [17, 21, 22]. Furthermore, the luminal subtype, among NGS-based classification subtypes, was recently reported to frequently show *ERBB2* gene alteration [23]. Thus, molecular subtype classification of UB UC is crucial for effective prognosis estimation and treatment planning.

In the mRNA-based subtype classification, high expression of *KRT5* is classified as the basal type and high expression of *KRT20* is classified as the luminal type [4, 5, 24, 25]. Accordingly, with IHC, the basal type shows high expression of CK5/6 and the luminal type shows high expression of CK20 [3, 5]. However, little has been published regarding cases in which both CK5/6 and CK20 showed high expression or in which neither protein showed high expression. In this study, two additional groups besides the basal and luminal types have been defined. These two groups are the double-positive type and double-negative type, for which we will investigate the molecular genetic characteristics. We could expect great clinical utility if two IHC assays could predict the molecular genetic characteristics of a tumor.

2. Materials and Methods

2.1. Tissue samples and case selection

In total, MIBC tissues from 30 patients who underwent a radical cystectomy at Seoul National University Hospital (SNUH) from 2016 to 2018 were included in this study. First, 30 fresh frozen tissue samples from 2016 to 2018 were investigated. The section containing prominent tumor tissue was selected, of which one section was prepared as a formalin-fixed paraffin-embedded (FFPE) tissue block, and the corresponding symmetric section was fresh frozen with liquid nitrogen and preserved in −70 ℃ until tumor excision. A total of 30 samples were classified to four subgroups based on IHC results for CK5/6 and CK20. In each subgroup three representative cases were selected, and RNA sequencing was carried out with a total of 12 fresh frozen tissue samples. All 12 patients were included in the prospective studies. Written informed consent was obtained from all patients enrolled in this mRNA analysis group.

Additionally, 189 MIBC patients who underwent transurethral resection of the bladder or radical cystectomy at SNUH or Seoul Metropolitan government-Seoul National University Boramae Medical Center were included in the survival analysis group. A total of 189 FFPE block tissue samples from 2004 to 2010 were investigated. A tissue microarray (TMA) block was prepared from FFPE tissue blocks (SuperBioChips Laboratories, Seoul, Republic of Korea). Two cores (2 mm in diameter) containing invasive tumor areas were obtained from each case. This study was approved by the Institutional Review Board (IRB) of SNUH (IRB No C-1701-083-823, 24 January 2017).

2.2. Immnohistochemistry

IHC for CK5/6, CK20, CK14, CD44, GATA3, FOXA1, p53, CD8 and HER2 was performed with an automatic immunostainer (BenchMark XT; Ventana Medical Systems, Tucson, AZ, USA), following the manufacturer's instructions. The primary antibodies against CK5/6 (1:100; D5/16 B4; Dako, Glostrup, Denmark), CK20 (1:50; Ks 20.8; Dako), CK14 (1:300; LL002; Cell Marque, Rocklin, CA, USA), CD44 (1:100; 156-3C11; Thermo Fisher, Waltham, MA, USA), GATA3 (L50-823; 1:500; Cell Marque), FOXA1 (1:500; PA5-27157; Thermo Fisher) and p53 (1:1000; DO7; Dako), CD8 (RTU; SP57; Ventana, Tucson, AZ, USA), HER2 (RTU; 4B5; Ventana) were used. And PD-L1 clone SP142 (Ventana Medical Systems; retrieval: CC1 48'; incubation: 16'; RTU dilution), clone SP263 (Ventana Medical Systems; retrieval: CC1 40'; incubation: 32'; ready to use [RTU] dilution) and clone 22C3 (Agilent Technologies, California; Dako Link-48 autostainer system) were used in accordance with the manufacturer's guidelines. Immunohistochemical positive control tissues were tonsil tissue for CK5/6 and CD44, duodenal mucosa epithelium for CK20, squamous cell carcinoma tissue for CK14, UC tissue for GATA3, gastric mucosa epithelium for p53, and breast cancer tissue, previously confirmed with positive expression for FOXA1. The SP142 and 22C3 assay used tonsil tissue and the SP263 assay used placenta tissue as control tissue. Two control tissues were used for each staining run, one as a positive control using an antibody reagent and one as a negative control using a negative reagent.

The full-section IHC staining was performed on all 12 cases, and in each case, two different invasive tumor areas were investigated. Additionally, the same IHC was carried out for 189 MIBC tissue TMA blocks.

For CK5/6, CK20, CK14, and CD44, >20% expression was defined as positive expression status. 20% cut-off value was reported in previous studies to be ideal for classification of

molecular subtypes in bladder cancer [16, 26]. So, we also applied the same criteria. GATA3 and FOXA1 were based on nuclear staining and percentage of stained cells and staining intensity were also considered. Staining intensity was scored to 0 to 3+ (0: no staining, 1+: weak staining, 2+: moderate staining, 3+: strong staining). 3+ staining intensity on more than 20% of tumor cells was defined as positive expression. p53 expression was measured by proportion of tumor cells with nuclear staining at any intensity. From the TMA cores, two noncontiguous areas with the highest CD8+ lymphocyte infiltration were chosen, and numbers of lymphocytes showing CD8 membranous staining were counted in per high power field (HPF) in both intra-tumoral and stromal compartment. For each case a mean value of four areas was obtained. Median score of all cases was set as a cut-off value, with which the cases were classified as high or low expression. HER2 protein expression was scored as 0, 1+, 2+, and 3+ according to the ASCO/CAP 2018 HER2 test guideline [27]. The average of the two core values was evaluated as the final result.

PD-L1 expression of tumor cells (TC) was evaluated based on the proportion of TC exhibiting membranous staining of any intensity. PD-L1 expression of immune cells (IC) was evaluated based on the proportion of tumor-associated IC with membranous, cytoplasmic, or punctate staining at any intensity and the proportion of tumor area that was occupied by PD-L1 staining IC of any intensity. Each PD-L1 expression type was dichotomized as "positive" or "negative" according to the manufacturer's recommendations. Cut-off criteria for PD-L1 expression positivity are summarized in Table 1.

Two pathologists (B.K. and C.L.) evaluated IHC staining at two different time points, without awareness of the previous results at the second evaluations. In the case of discrepant results between evaluations another pathologist (K.C.M) was consulted before making the final decision.

Table 1. Positive criteria of PD-L1 assays.

	Cutoff for positivity
PD-L1 (SP142)	Presence of discernible PD-L1 staining of any intensity in tumor-infiltrating immune cells covering > 5% of tumor area occupied by tumor cells, associated intratumoral, and contiguous peritumoral stroma
PD-L1 (SP263)	≥ 25% of tumor cells exhibit membrane staining; or, ICP > 1% and IC+ ≥ 25%; or, ICP = 1% and IC+ = 100%
PD-L1 (22C3)	CPS ≥10; CPS= $\frac{\text{PD-L1 staining cells (tumor cells, lymphocytes, macrophages)}}{\text{Total number of viable tumor cells}}$ x 100

Abbreviations: CPS, Combined positive score; IC+, Percentage of tumor-associated immune cells with staining; ICP, Immune cells present (percent of tumor area occupied by any tumor-associated immune cells).

2.3. RNA sequencing

After IHC results were identified on the FFPE tissue block, mRNA was extracted from the corresponding location of the symmetric fresh-frozen MIBC tissues. A 3-mm-sized plunger was used for punching out the fresh-frozen tissue. RNA library was assembled with TruSeq RNA Access Library Prep Kit, and base sequence analysis was carried out with Illumina HiSeq 2500 platform (Illumina, San Diego, CA, USA). (Macrogen, Inc., Seoul, Korea) Paired demultiplexed fastq files were generated, and initial quality control was performed using FastQC (Phred quality score >30). The adaptor sequences were removed by using Trimmomatic program and trimmed data were mapped to the reference genome (UCSC hg19) using the HISAT2 and Bowtie2. Previously known gene/transcripts were assembled with the StringTie program. Raw data were normalized and, mRNA expression data were presented as reads transcript per million and were transformed into log 2 volume values for the analysis.

2.4. Functional analysis

In this study, differential expression genes (DEGs) were identified with DESeq2. Statistical analysis was performed on selected genes whose median count for each gene was greater than 5 in at least one comparison combination. Functional analysis of DEGs was performed using Gene ontology (GO) and the Kyoto Encyclopedia of Genes and Genomes (KEGG) pathway (adjusted p-value <0.05 and |fold change| ≥2). The analyses were performed by biological process, molecular function, and cellular component, which are the GO subcategories. Functional annotation based on the KEGG database was implemented. Additionally, the functional analyses were performed with the use of Ingenuity pathway analysis (IPA).

2.5. Statistical analysis

The association between IHC-defined subgroups with IHC expression was evaluated by the chi-squared test. The comparison analysis of CD8+ lymphocyte numbers between IHC-defined subgroups was performed using Mann-Whitney test. The associations between IHC-subgroups and progression-free survival (PFS), and overall survival (OS) were evaluated by the Kaplan-Meier method with the log-rank test. The concordance rate of PD-L1 expression between the SP142 assay, the SP263 assay and the 22C3 assay was evaluated. Cohen's kappa coefficient of agreement was calculated: the level of concordance could be classified as poor (kappa=0.00), slight (kappa=0.00-0.20), fair (kappa=0.21-0.40), moderate (kappa=0.41-0.60), substantial (kappa=0.61-0.80) or almost perfect (kappa=0.81-1.00) [28]. Statistical analyses were performed using SPSS software (version 23; IBM, Armonk, NY, USA). Two-sided p-values < 0.05 were considered to be statistically significant.

3. Results

3.1. Subgroup classification of RNA sequencing group

Thirty cases of MIBC in patients who underwent a radical cystectomy between 2016 and 2018 and for whom we were able to acquire fresh frozen tissues were included. With these samples, we subdivided the cases into four subgroups based on CK5/6 and CK20 IHC expression. The CK5/6 single-positive (CK5/6 SP) subgroup was CK5/6 ^{high}/CK20 ^{low}, the CK20 single-positive (CK20 SP) subgroup was CK5/6 ^{low}/CK20 ^{high}, the double-positive (DP) subgroup was CK5/6 ^{high}/CK20 ^{high} and the double-negative (DN) was CK5/6 ^{low}/CK20 ^{low}. Six cases of the CK5/6 SP subgroup, 10 cases of the CK20 SP subgroup, nine cases of the DP subgroup and five cases of the DN subgroup were identified (Figure 1).

Three cases were selected from each subgroup, and mRNA sequencing was performed on fresh frozen tissue samples of 12 patients. The mean age of patients was 68.7 years (range, 55–83) at diagnosis, and the male-to-female sex ratio was 10:2. Seven patients were in stage IIIA and five patients were in stage IIIB according to the 8th edition of the TNM staging system of the American Joint Committee on Cancer (AJCC) [29]. Lymph node metastasis was found in six cases. All 12 cases were classified as high grade according to the World Health Organization/ International Society of Urologic Pathologists (WHO/ISUP) grading system [30].

We additionally performed CD44, CK14, GATA3, FOXA1 and p53 IHC in 12 cases. In CD44, a basal-type marker, IHC expression was positive in all CK5/6 SP and DP subgroup cases and mostly negative in CK20 SP and DN subgroups. In CK14, another basal-type marker, IHC expression was positive in one case in the DP subgroup and two cases in the CK5/6 SP subgroup and was negative in all remaining cases. In GATA3, a luminal-type marker, IHC expression was positive in all three CK20 SP subgroup cases and negative in all three CK5/6 SP subgroup cases. FOXA1 IHC

expression was positive in two cases in the CK20 SP subgroup and one case in the DN subgroup and was negative in all remaining cases, including CK5/6 SP and DP subgroup cases. p53 IHC expression showed a wide range from negative to greater than 95% positive expression.

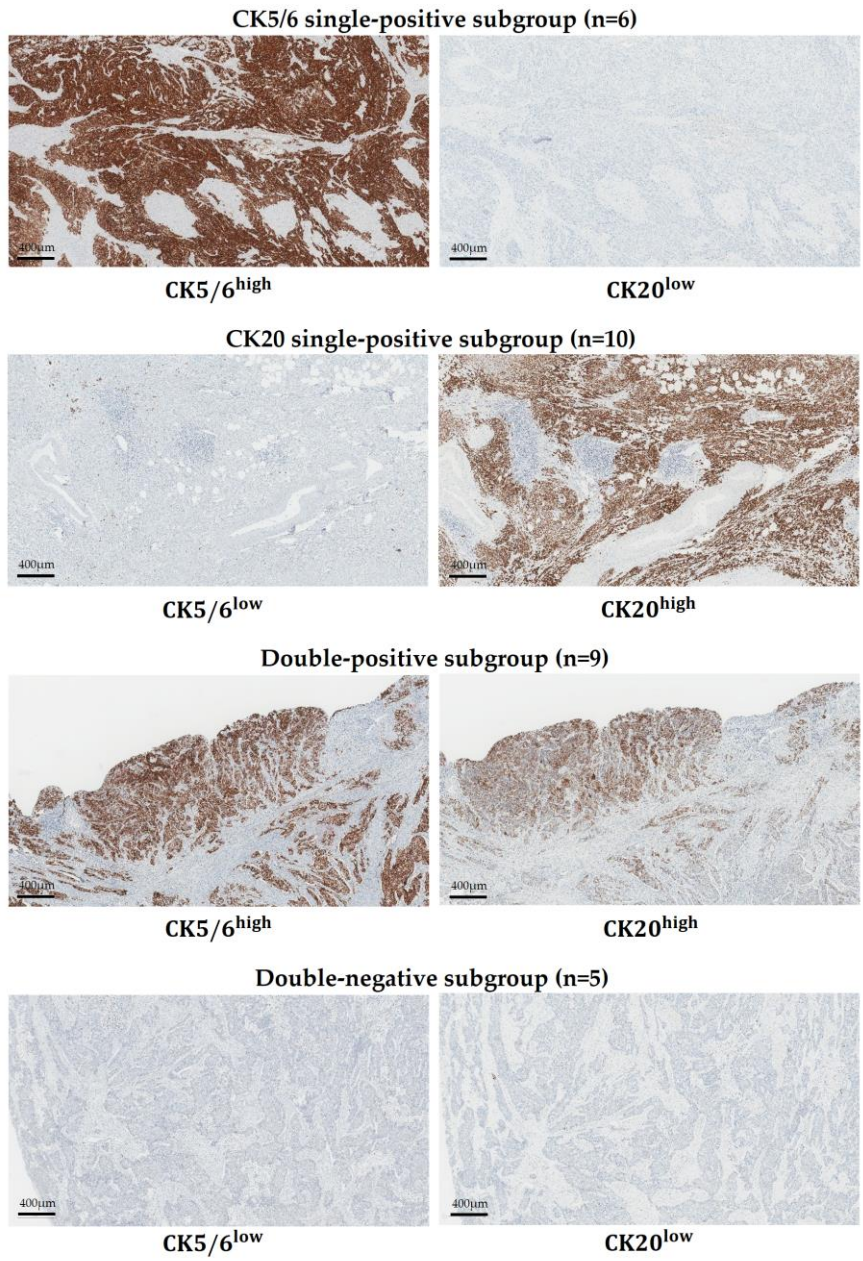

Figure 1. Subgrouping of MIBC by CK5/6 and CK20 immunohistochemistry

3.2. Differential expression genes between each subgroup

RNA sequencing data were analyzed from 12 MIBC tissues. Using adjusted p−value <0.05 and |fold change| ≥2 as the cut−offs, we identified 38 DEGs between the DP and CK20 SP subgroups, 98 DEGs between the DP and CK5/6 SP subgroups, 433 DEGs between the DP and DN subgroups, 183 DEGs between the CK20 SP and CK5/6 SP subgroups, 256 DEGs between the CK20 SP and DN subgroups, and 614 DEGs between the CK5/6 SP and DN subgroups. In total, 1062 DEGs were identified. Compared with the DP, CK5/6, and DN subgroups, the CK20 SP subgroup had 10, 77, and 174 upregulated genes, respectively, and 28, 106 and 82 downregulated genes, respectively. Compared with the DP and CK 20 SP and the DN subgroups, the CK5/6 SP subgroup had 43, 106, and 429 upregulated genes, respectively, and 55, 77, and 185, downregulated genes, respectively. Compared with the DP, CK20 SP and CK5/6 SP subgroups, the DN subgroup had 79, 82 and 185 upregulated genes, respectively, and 354, 174 and 429 downregulated genes, respectively. A Venn diagram of DEGs in the four major comparison conditions is shown in Figure 2.

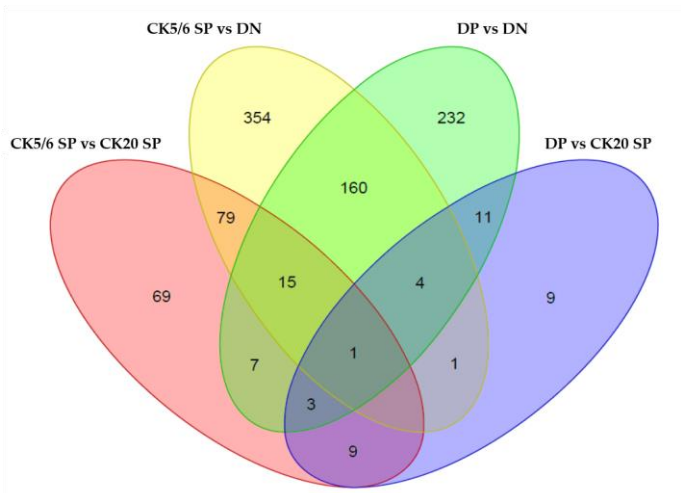

Figure 2. Venn diagram of DEGs in four major comparison conditions.

3.3. Gene ontology analysis

The results of GO analysis between each subgroup are summarized in Table 2. Between the CK5/6 SP and CK20 SP subgroups, the leukocyte aggregation GO term was identified. Some related DEGs (*S100A9, CD44* and *S100A8*) were upregulated in the CK5/6 SP subgroup. Between the CK5/6 SP and DN subgroups, various GO terms related to immune response and the tumor necrosis factor (TNF) signaling pathway were identified, and various related DEGs (*CD86, HLA-DMB, CD209, CCL19, TLR1, BTK, IRAK3* and *TLR 6*) were upregulated in the CK5/6 SP subgroup. Between the DP and CK20 SP subgroups, GO terms related to immune response were identified, and various related DEGs (*CCL4L1, S100A9, IL1B* and *LILRB1*) were upregulated in the DP subgroup. Between the DP and DN subgroups, GO terms related to cell proliferation, immune response, mitogen-activated protein kinase (MAPK) signaling pathway and TNF signaling pathway were identified, and various related DEGs (*CCL14, CD74, CD4, CD86, FLT3* and *LRRK2*) were upregulated in the DP subgroup.

When comparing the CK5/6-positive and CK5/6-negative groups, we identified 226 DEGs. Compared to the CK5/6-negative group, the CK5/6-positive group had 169 upregulated genes and 57 downregulated genes. The CK5/6-positive group was enriched with cell migration, immune response, MAPK signaling pathway and TNF signaling pathway associated GO terms. Compared to CK5/6-negative tumors, many DEGs (*ACVR1, CSF1R, SEMA4A, SASH3, CD74, HLA-DMB, TLR1, BTK, IRAK3, MAP4K1* and *CD40*) associated with previously mentioned GO terms were upregulated in CK5/6-positive group tumors (Table 3).

Table 2. The GO analysis results between each subgroup.

CK5/6 SP vs. DP
None related to major cellular function
CK5/6 SP vs. CK20 SP
Immune response (leukocyte aggregation)
CK5/6 SP vs. DN
Immune response (positive regulation of lymphocyte proliferation, positive regulation of T cell activation, positive regulation of T cell proliferation, regulation of B cell receptor signaling pathway, neutrophil activation involved in immune response, and positive regulation of leukocyte cell−cell adhesion) TNF signaling pathway (MyD88−dependent toll−like receptor signaling pathway and positive regulation of NF− κB transcription factor activity)
DP vs. CK20 SP
Immune response (regulation of T cell proliferation and positive regulation of inflammatory response)
DP vs. DN
Cell proliferation (positive regulation of cell proliferation) Immune response (T cell proliferation, regulation of T cell activation, regulation of immune response, regulation of inflammatory response, regulation of B cell proliferation, positive regulation of lymphocyte proliferation, positive regulation of T cell activation, and positive regulation of T cell proliferation) TNF signaling pathway (positive regulation of tumor necrosis factor biosynthetic process, positive regulation of tumor necrosis factor production, regulation of tumor necrosis factor biosynthetic process, MyD88−dependent toll−like receptor signaling pathway, positive regulation of I− κB kinase/NF− κB signaling, regulation of I− κB kinase/NF− κB signaling, regulation of interleukin−6 production, and regulation of interleukin−8 secretion) MAPK signaling pathway (activation of MAPK activity, regulation of MAP kinase activity, positive regulation of MAP kinase activity, positive regulation of MAPK cascade, positive regulation of phosphatidylinositol 3−kinase signaling, positive regulation of ERK1 and ERK2 cascade, regulation of ERK1 and ERK2 cascade, and positive regulation of JNK cascade)
CK20 SP vs. DN
None related to major cellular function

Abbreviations: CK5/6 SP, CK5/6 single−positive; CK20 SP, CK20 single−positive; DN, double−negative; DP, double−positive; NF− κB, Nuclear factor− κB; TNF, Tumor necrosis factor.

Table 3. The GO analysis results between CK5/6 positive and CK5/6 negative group.

CK5/6−Positive vs. CK5/6−Negative
Cell migration (positive regulation of cell migration, positive regulation of cell motility, and regulation of cell migration)
Immune response (positive regulation of immune response, positive regulation of inflammatory response, positive regulation of lymphocyte proliferation, regulation of immune response, regulation of immune response, B cell activation, regulation of B cell proliferation, positive regulation of T cell activation, regulation of T cell proliferation, and T cell activation)
TNF signaling pathway (positive regulation of NF−κB transcription factor activity and MyD88−dependent toll−like receptor signaling pathway)
MAPK signaling pathway (positive regulation of MAP kinase activity, positive regulation of MAPK cascade, regulation of MAP kinase activity, regulation of ERK1 and ERK2 cascade, and positive regulation of JNK cascade)

3.4. Ingenuity Pathways Analysis and Gene set enrichment analysis

The IPA results showed that some functions related to immune response and cell migration were activated in the CK5/6 SP and DP subgroups (Table 4). Regulator effect analysis also indicated analogous results (Figure 3). The significant ingenuity canonical pathways of DEGs between four subgroups are listed in Figure 4.

Gene set enrichment analysis (GSEA) confirmed that the interleukin 6-Janus kinase-signal transducer and activator of transcription 3 (IL6-JAK-STAT3) signaling pathway, inflammatory response and TNF-α signaling via nuclear factor-κB (NF-κB) signaling pathway were significantly enriched in the DP and CK5/6 SP subgroups. (Figure 5) However, in the comparison conditions of the CK5/6 SP and CK20 SP subgroups, related functions did not exhibit a significant difference.

Table 4. The IPA results (disease and function).

CK5/6 SP vs. DP	
	None related to major cellular function
CK5/6 SP vs. CK20 SP	
upregulated in CK5/6 SP	Cancer and invasion of tumor cell lines Adhesion of immune cells
CK5/6 SP vs. DN	
upregulated in CK5/6 SP	Cancer, neoplasia of cells, cell movement of cancer cells, cell movement of tumor cell lines, cell movement, and migration of cells Lymphocyte migration, cell movement of T lymphocytes, leukocyte migration, cell movement of mononuclear leukocytes, activation of lymphocytes, proliferation of immune cells, and proliferation of lymphocytes
DP vs. CK20 SP	
upregulated in DP	Activation of leukocytes, activation of mononuclear leukocytes, and leukocyte migration Chemotaxis
DP vs. DN	
upregulated in DP	Cancer and activation of cells Cell movement, migration of cells, and binding of tumor cell lines Activation of lymphocytes, lymphocyte migration, cell movement of lymphocytes, immune response of cells, and inflammatory response I−κB kinase/NF−κB cascade
CK20 SP vs. DN	
upregulated in CK20 SP	Activation of cells

Abbreviations: CK5/6 SP, CK5/6 single−positive; CK20 SP, CK20 single−positive; DN, double−negative; DP, double−positive.

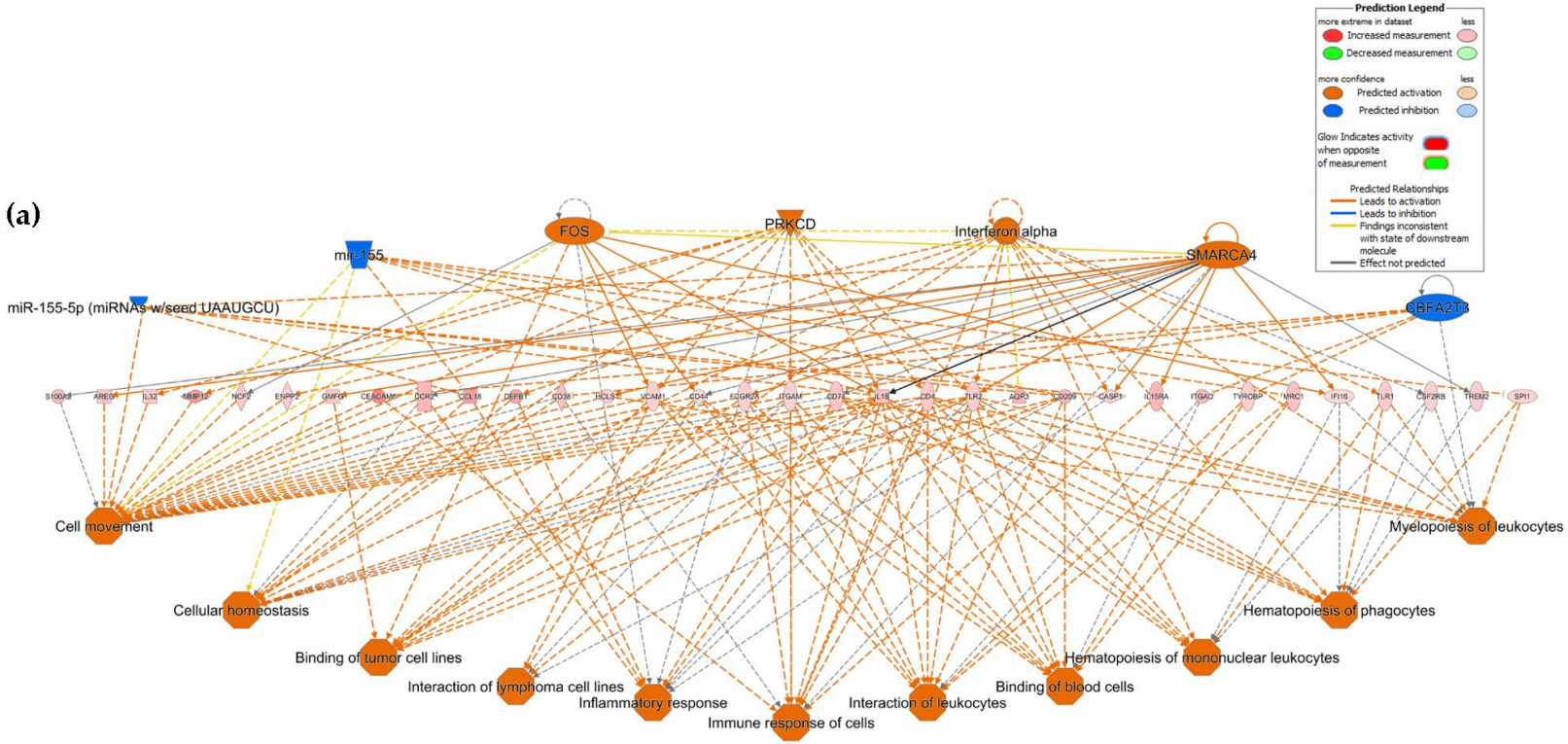
(a)
Prediction Legend
more extreme in dataset
less
Increased measurement
Decreased measurement
more confidence
less
Predicted activation
Predicted inhibition
Glow Indicates activity when opposite of measurement
Predicted Relationships
Leads to activation
Leads to inhibition
Findings inconsistent with state of downstream molecule
Effect not predicted
FOS
PRKCD
Interferon alpha
SMARCA4
mir-155
miR-155-5p (miRNAs w/seed UAAUGCU)
CBFA2T3
Cell movement
Myelopoiesis of leukocytes
Cellular homeostasis
Hematopoiesis of phagocytes
Binding of tumor cell lines
Hematopoiesis of mononuclear leukocytes
Interaction of lymphoma cell lines
Inflammatory response
Interaction of leukocytes
Binding of blood cells
Immune response of cells

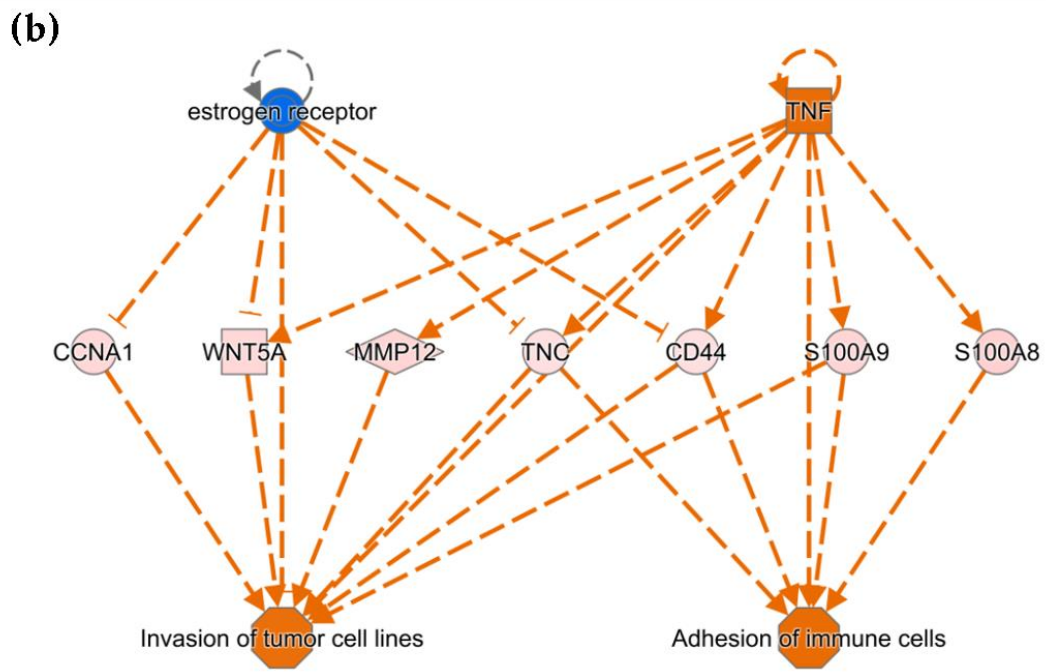
(b)
estrogen receptor
TNF
CCNA1
WNT5A
MMP12
TNC
CD44
S100A9
S100A8
Invasion of tumor cell lines
Adhesion of immune cells

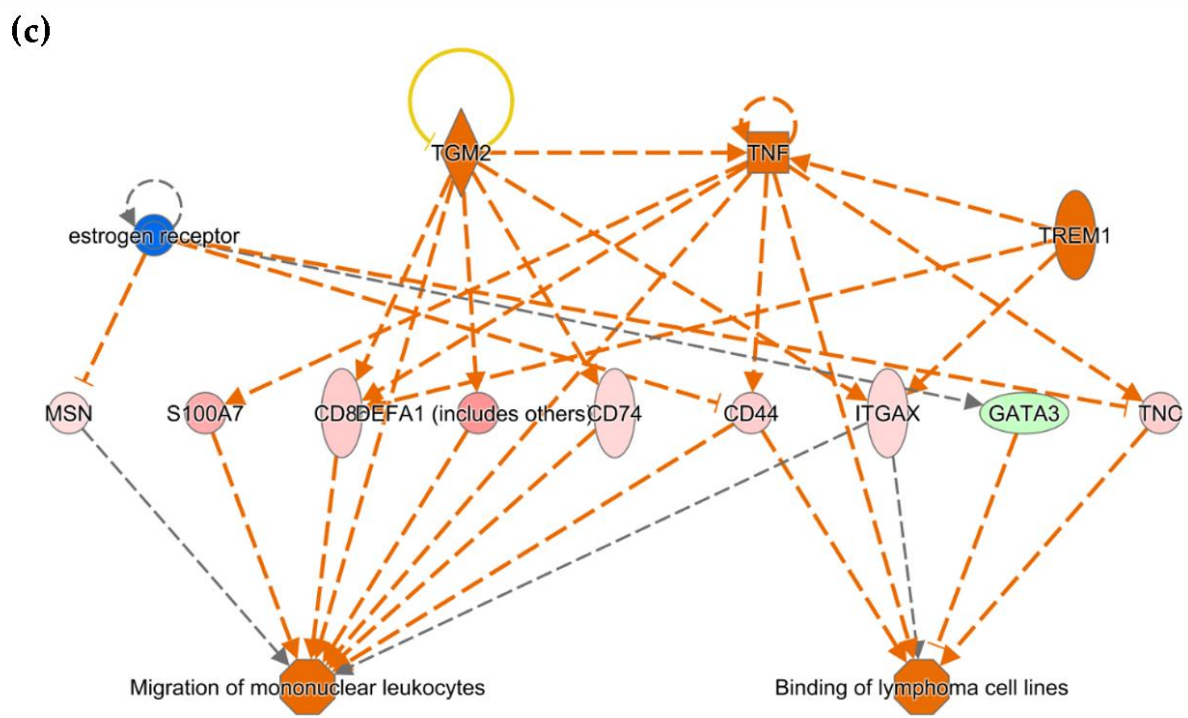
(c)
TGM2
TNF
estrogen receptor
TREM1
MSN
S100A7
CD8B
DEFA1 (includes others)
CD74
CD44
ITGAX
GATA3
TNC
Migration of mononuclear leukocytes
Binding of lymphoma cell lines

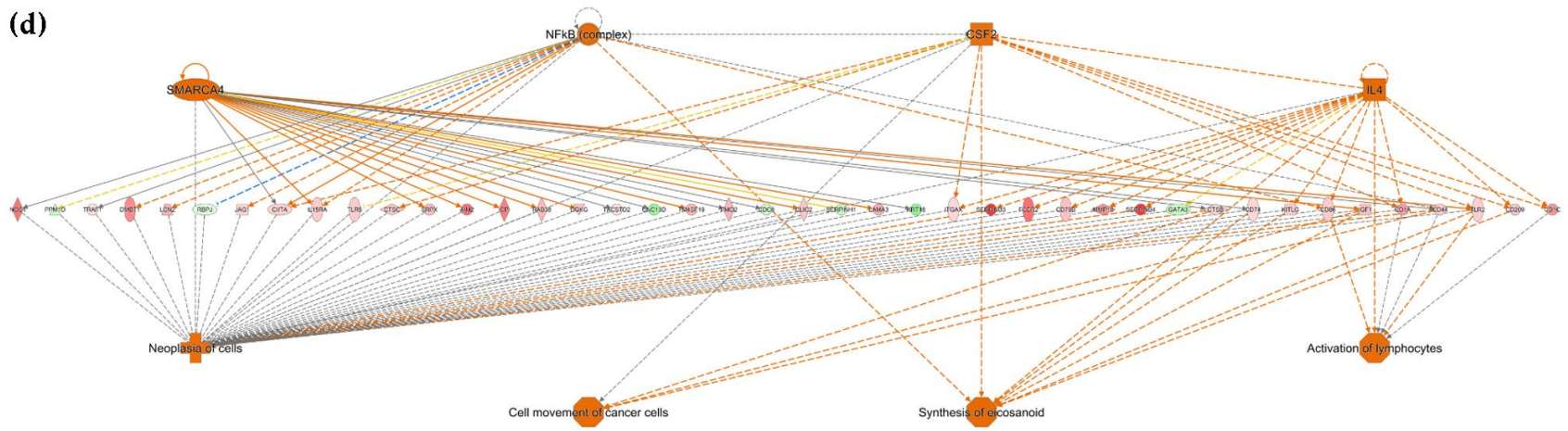

Figure 3. The IPA results; Regulator effect between four subgroups: (a) DP vs DN; (b) CK5/6 SP vs CK20 SP; (c) CK5/6 SP vs DN; (d) CK5/6 SP vs DN.

Figure 4. The ingenuity canonical pathways of DEGs between four subgroups: (a) CK5/6 SP vs. DN; (b) CK5/6 SP vs. CK20 SP; (c) DP vs. DN; (d) DP vs. CK20 SP; (e) CK5/6 SP vs. DP; (f) DN vs. CK20 SP.

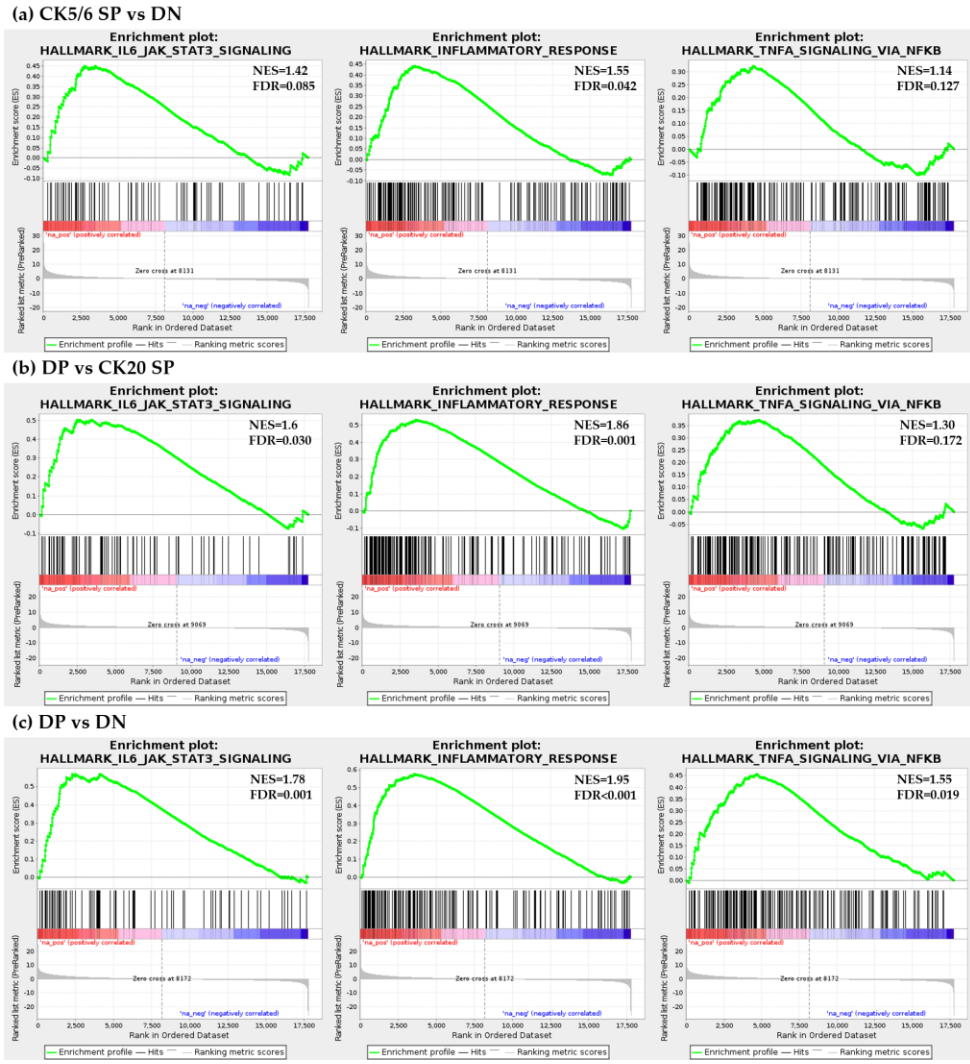

Figure 5. The GSEA results: (a) CK5/6 SP vs. DN; (b) DP vs. CK20 SP; (c) DP vs. DN.

3.5. Expression of gene signature markers

We compared the expression patterns of gene signature markers between four subgroups (Figure 6). Expression of basal-type markers was most enriched in the CK5/6 SP subgroup, and the DP, CK20 SP, and DN subgroups followed in respective order. In contrast, expression of luminal-type markers was most enriched in the CK20 SP subgroup, and the DP, DN, and CK5/6 SP subgroups followed in respective order. Expression of p63-associated genes was the highest in the CK5/6 SP subgroup followed by the DP subgroup, and the CK20 SP and DN subgroups showed low expression. Expression of TP53-like signature genes was lowest in the DN subgroup. Expression of immune cell-associated genes was highest in the DP subgroup. Compared with the CK5/6-negative group, expression of epithelial-mesenchymal transition (EMT) markers was enriched in the CK5/6-positive group. Expression of cell adhesion markers was enriched to the highest degree mostly in the CK5/6 SP subgroup, which was followed by the DP subgroup. Expression was relatively low in the remaining CK5/6-negative group. Expression of TNF and MAPK signaling pathway was enriched in the DP and CK5/6 SP subgroups. The DN subgroup showed the lowest expression.

(a) basal type genes

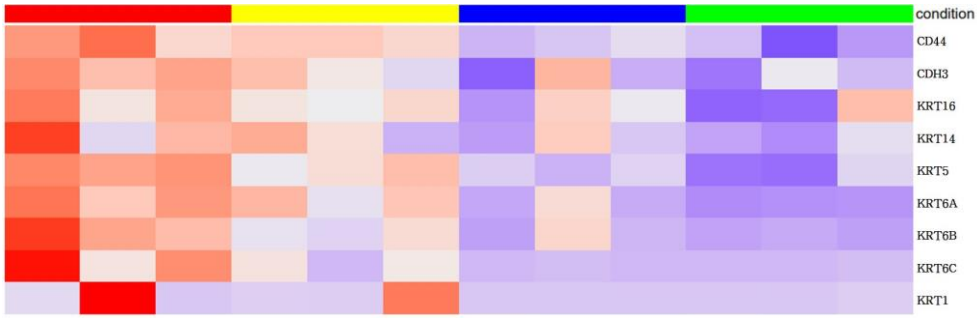

(b) luminal type genes

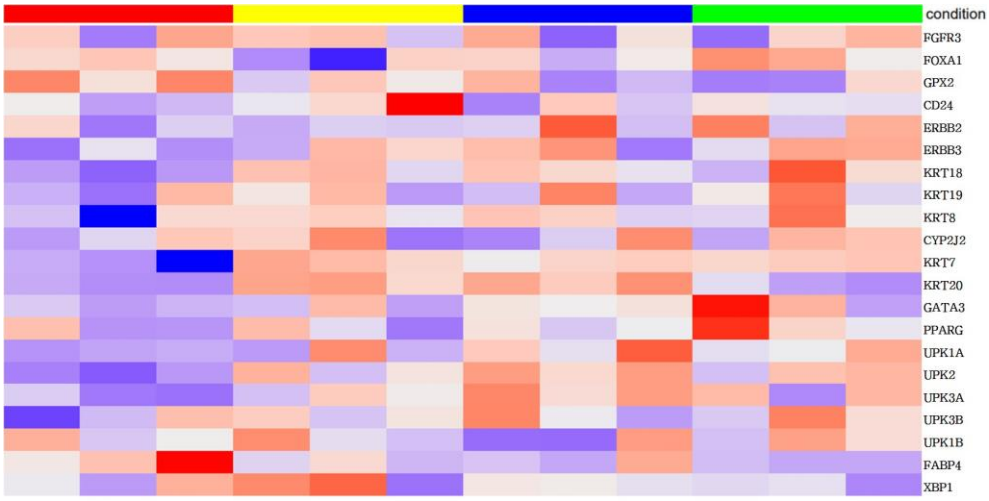

(c) p63-associated genes

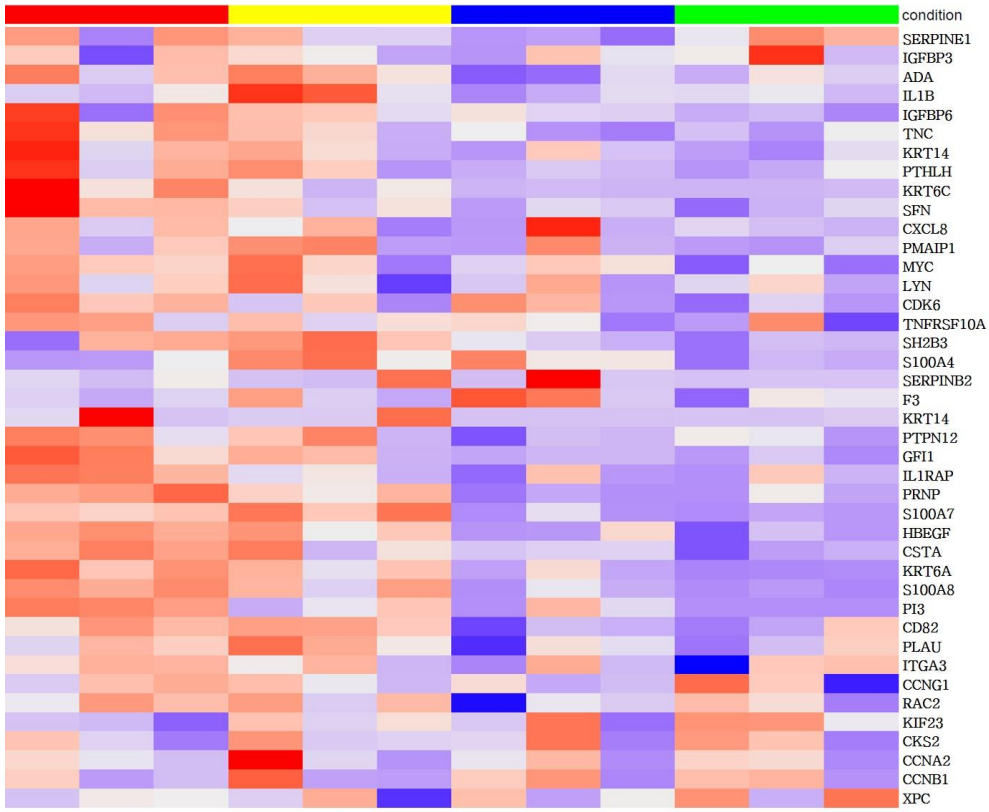

(d) TP53-like signature genes

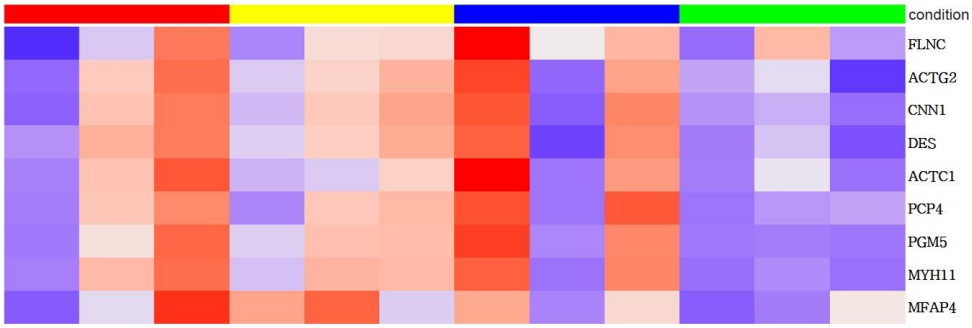

(e) immune response genes

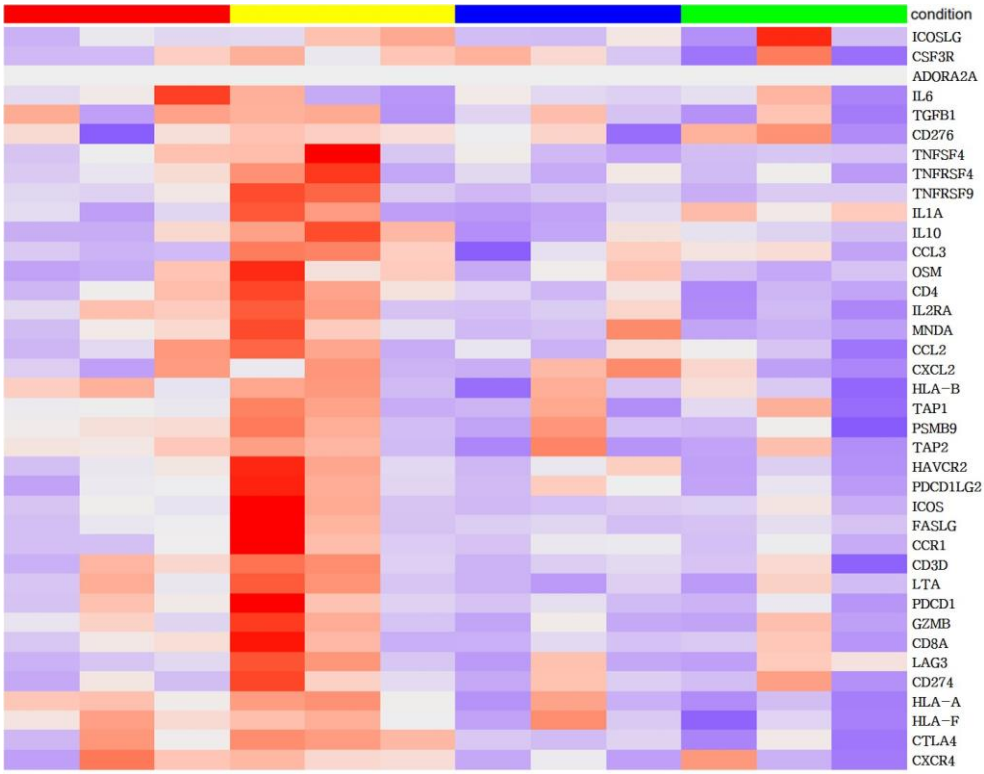

(f) epithelial-mesenchymal transition genes

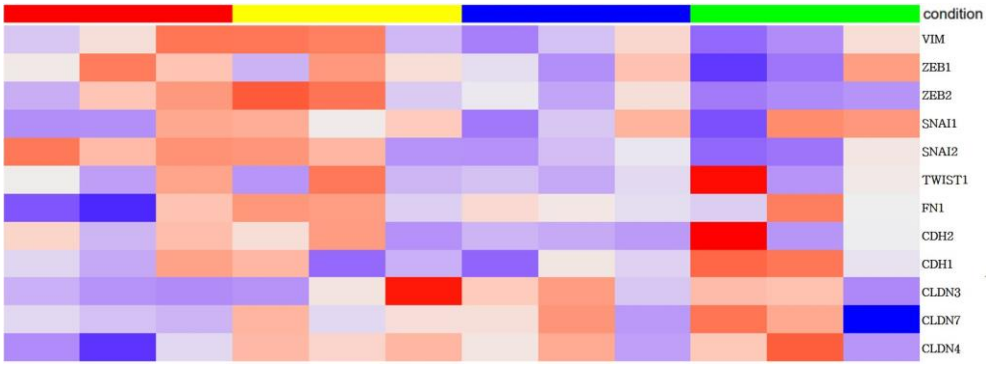

(g) cell adhesion genes

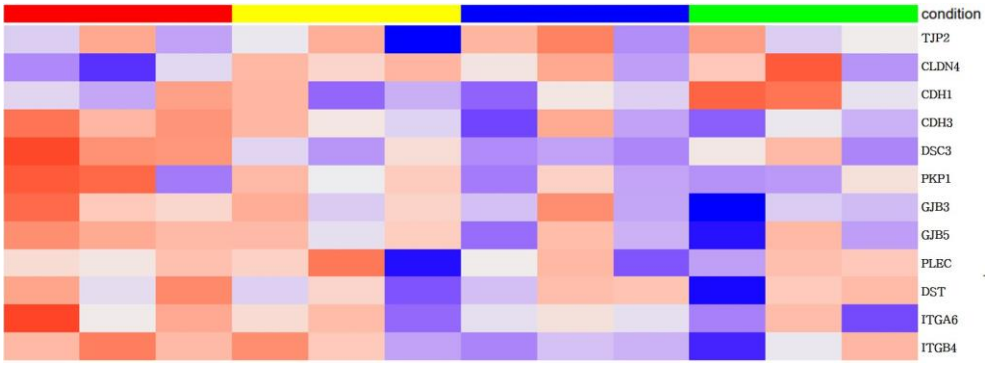

(h) MAPK signaling pathway genes

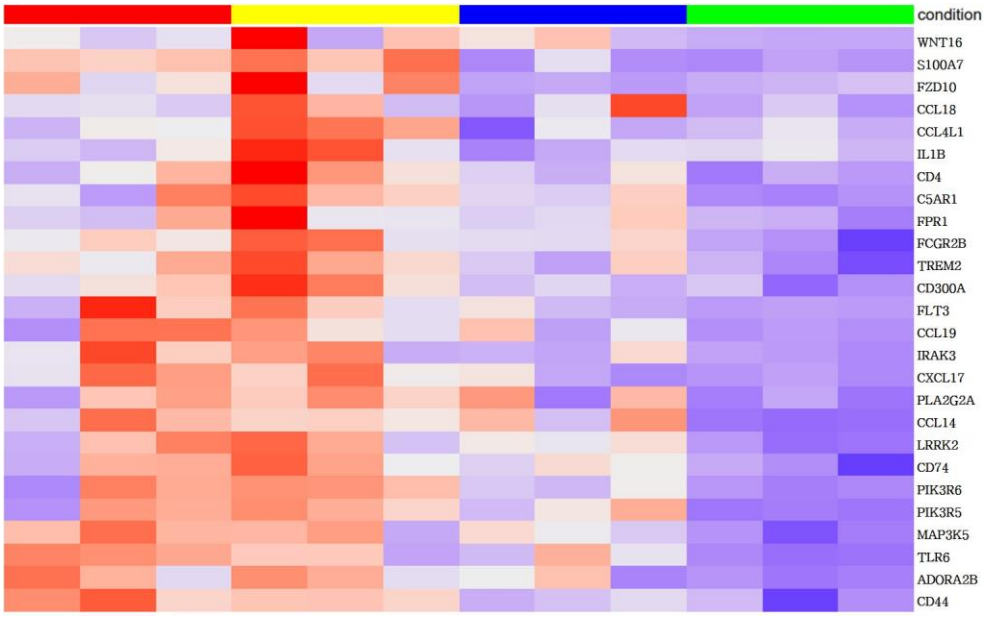

(i) TNF signaling pathway genes

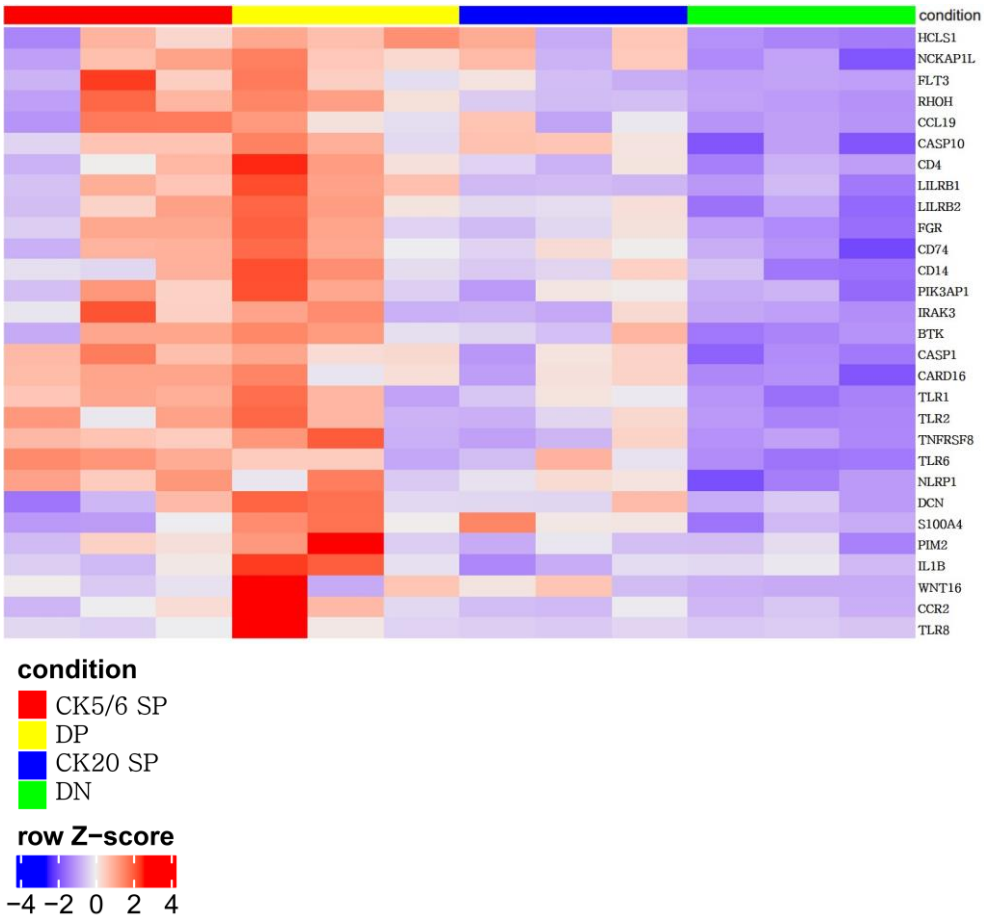

Figure 6. Expression of gene expression signature between four subgroups: (a) basal type genes; (b) luminal type genes; (c) p63-associated genes; (d) TP53-like signature genes; (e) immune response genes; (f) epithelial-mesenchymal transition genes; (g) cell adhesion genes; (h) MAPK signaling pathway genes; (i) TNF signaling pathway genes.

3.6. Clinicopathological analysis of IHC-based subgroups

The clinicopathological and demographic characteristics of the 189 patients for whom we performed IHC analysis are summarized in Table 5. Overall, 189 patients were included in this study, including 158 men and 31 women. The age of the patients ranged from 37 to 87 years with a mean age of 68 years. According to the 8th edition of the TNM staging system of the AJCC, 172 patients were in pT2, 10 patients were in pT3, and 7 patients were in pT4. According to the WHO/ISUP grading system, seven cases were classified as low grade, and 182 cases were classified as high grade. Only conventional UB UC cases were selected excluding specific variant cases. IHC was performed to subdivide subgroups, and the results were as follows. There were 61 cases in the CK5/6 SP subgroup, 13 cases in the DP subgroup, 70 cases in the CK20 SP subgroup and 45 cases in the DN subgroup that were confirmed. (Table 6).

Table 5. Clinicopathological characteristics of patients and association with IHC-defined subgroups.

	CK5/6 SP	DP	CK20 SP	DN	Total
	n (%)	*n* (%)	*n* (%)	*n* (%)	*n*
Age (years)					
≤68	27 (44.3%)	7 (53.8%)	29 (41.4%)	21 (46.7%)	84
>68	34 (55.7%)	6 (46.2%)	41 (58.6%)	24 (53.3%)	105
Gender					
Male	48 (78.7%)	13 (100%)	58 (82.9%)	39 (86.7%)	158
Female	13 (21.3%)	0 (0.0%)	12 (17.1%)	6 (13.3%)	31
Nuclear grade					
Low	1 (1.6%)	0 (0.0%)	3 (4.3%)	3 (6.7%)	7
High	60 (98.4%)	13 (100%)	67 (95.7%)	42 (93.3%)	182
T category					
T2	55 (90.2%)	12 (92.3%)	63 (90.0%)	42 (93.3%)	172
T3~4	6 (9.8%)	1 (1.1%)	7 (10.0%)	3 (6.7%)	17

Abbreviations: CK5/6 SP, CK5/6 single-positive; CK20 SP, CK20 single-positive; DN, double-negative; DP, double-positive; IHC, immunohistochemistry.

Table 6. Relationship between IHC-defined subgroups with immunohistochemistry expression.

	CK5/6 SP	DP	CK20 SP	DN	Total
	n (%)	*n* (%)	*n* (%)	*n* (%)	*n*
CK14					
Low	28 (45.9%)	12 (92.3%)	69 (98.6%)	45 (100%)	154
High	33 (54.1%)	1 (7.7%)	1 (1.4%)	0 (0.0%)	35
CD44					
Low	2 (3.3%)	2 (15.4%)	64 (91.4%)	34 (75.6%)	102
High	59 (96.7%)	11 (84.6%)	6 (8.6%)	11 (24.4%)	87
GATA3					
Low	55 (90.2%)	3 (23.1%)	11 (15.7%)	20 (44.4%)	89
High	6 (9.8%)	10 (76.9%)	59 (84.3%)	25 (55.6%)	100
FOXA1					
Low	56 (91.8%)	9 (69.2%)	25 (35.7%)	30 (66.7%)	120
High	5 (91.8%)	4 (30.8%)	45 (64.3%)	15 (33.3%)	69

Abbreviations: CK5/6 SP, CK5/6 single-positive; CK20 SP, CK20 single-positive; DN, double-negative; DP, double-positive; IHC, immunohistochemistry.

3.7. PD-L1 assays

The results of the SP142, SP263 and 22C3 assays are summarized in Table 7. The overall concordance rate for PD-L1 expression between SP 142 and SP 263 was 89.4%. (169/189) (kappa =0.681) The overall concordance rate for PD-L1 expression between SP 142 and 22C3 was 91.0%. (172/189) (kappa =0.700) The overall concordance rate for PD-L1 expression between SP 263 and 22C3 was 94.2%. (178/189) (kappa =0.836) The SP142 assay showed 15.9% (30/189) positivity, at the IC 5% cutoff. The mean percentage of IC expression was 2.6% (range, 0-80) and the mean percentage of TC expression was 2.8 % (range, 0-80). The SP263 assay showed 25.4% (48/189) positivity at the TC or IC 25% cutoff. When further subdivided, 14 cases met only the TC criteria, 12 cases met only the IC criteria, and 22 cases met both TC and IC criteria. The mean percentage of IC expression was 9.6% (range, 0-80) and the mean percentage of TC expression was 11.4% (range, 0-95) and). The 22C3 assay showed 20.6% (39/189) positivity, at the Combined Positive Score (CPS) 10 cutoff. The mean CPS was 5.9% (range, 0-90).

The union with either SP142 or SP263 or 22C3 assays positive cases was 50 cases. A Venn diagram of DEGs in the PD-L1 assays positive cases is shown in Figure 7. All but one of 30 cases positive for the SP142 assay were also positive for the SP263 assay, and all but one of 39 cases positive for the 22C3 assay were also positive for the SP263 assay.

Comparisons of PD-L1 IHC expression with the SP142, SP263 and 22C3 assays between positive and negative groups classified according to CK5/6, CK14, CD44, CK20, GATA3 and FOXA1 expression levels are summarized in Table 8. High positivity in all the SP142, SP263 and 22C3 assays was significantly correlated with positive CK5/6, positive CK14, positive CD44, negative CK20 negative GATA3 and negative FOXA1 expression.

Table 7. Distribution of PD-L1 expression in MIBC.

PD-L1 assay	Positive cell	Positive rate					
		0%	1-4%	5-9%	10-24%	25-49%	50-100%
SP142	TC	137 (72.5%)	23 (12.2%)	11 (5.8%)	11 (5.8%)	5 (2.6%)	2 (1.1%)
	IC	96 (50.8%)	63 (33.3%)	12 (6.3%)	14 (7.4%)	2 (1.1%)	2 (1.1%)
SP263	TC	108 (57.1%)	25 (13.2%)	10 (5.3%)	10 (5.3%)	16 (8.5%)	20 (10.6%)
	IC	67 (35.4%)	44 (23.3%)	23 (12.2%)	21 (11.1%)	25 (13.2%)	9 (4.8%)
22C3	CPS	100 (52.9%)	32 (16.9%)	18 (9.6%)	24 (12.7%)	10 (5.3%)	5 (2.6%)

Abbreviations: CPS, Combined positive score; IC, immune cell; MIBC, Muscle-invasive urinary bladder urothelial cell carcinoma; TC, tumor cell.

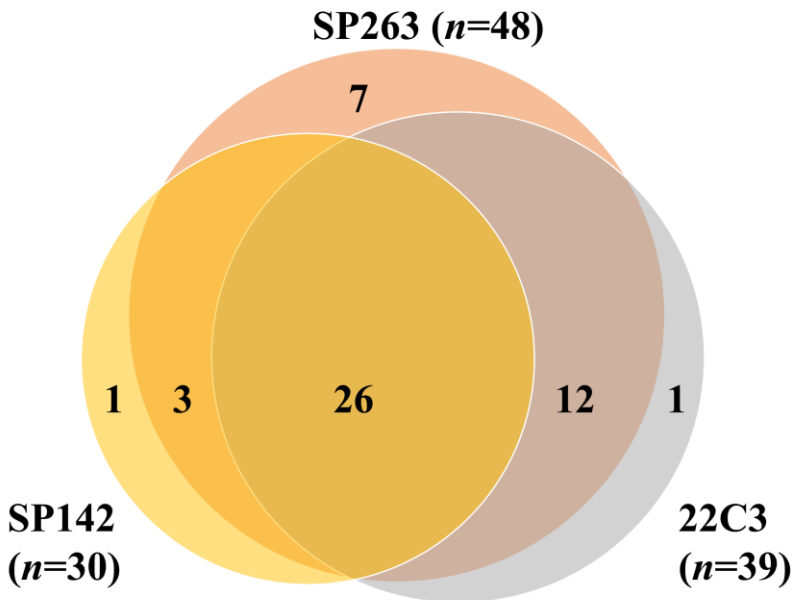

Figure 7. Venn diagram of DEGs in the PD-L1 assays positive cases.

Table 8. Relationship between PD-L1 positivity and CK5/6, CK14, CD44, CK20, GATA3 and FOXA1 expression.

		SP142			SP 263			22C3		
		Negative	Positive	*p*-Value	Negative	Positive	*p*-Value	Negative	Positive	*p*-Value
CK5/6	Neg	109 (68.6%)	6 (20.0%)	<0.001	107 (75.9%)	8 (16.7%)	<0.001	108 (72.0%)	7 (17.9%)	<0.001
	Pos	50 (31.4%)	24 (80.0%)		34 (24.1%)	40 (83.3%)		42 (28.0%)	32 (82.1%)	
CK14	Neg	137 (86.2%)	17 (56.7%)	<0.001	129 (91.5%)	25 (52.1%)	<0.001	132 (88.0%)	22 (56.4%)	<0.001
	Pos	22 (13.8%)	13 (43.3%)		12 (8.5%)	23 (47.9%)		18 (12.0%)	17 (43.6%)	
CD44	Neg	98 (61.6%)	4 (13.3%)	<0.001	96 (68.1%)	6 (12.5%)	<0.001	97 (64.7%)	5 (12.8%)	<0.001
	Pos	61 (38.4%)	26 (86.7%)		45 (31.9%)	42 (87.5%)		53 (35.3%)	34 (87.2%)	
CK20	Neg	79 (49.7%)	27 (90.0%)	<0.001	63 (44.7%)	43 (89.6%)	<0.001	71 (47.3%)	35 (89.7%)	<0.001
	Pos	80 (50.3%)	3 (10.0%)		78 (55.3%)	5 (10.4%)		79 (52.7%)	4 (10.3%)	
GATA3	Neg	66 (41.5%)	23 (76.7%)	<0.001	50 (35.5%)	39 (81.3%)	<0.001	58 (38.7%)	31 (79.5%)	<0.001
	Pos	93 (58.5%)	7 (23.3%)		91 (64.5%)	9 (18.8%)		92 (61.3%)	8 (20.5%)	
FOXA1	Neg	94 (59.1%)	26 (86.7%)	0.004	79 (56.0%)	41 (85.4%)	<0.001	86 (57.3%)	34 (87.2%)	0.001
	Pos	65 (40.9%)	4 (13.3%)		62 (44.0%)	7 (14.6%)		64 (42.7%)	5 (12.8%)	

Abbreviations: Neg, negative; Pos, positive.

3.8. PD-L1 expression in IHC-based subgroups

Most of the all the SP142, SP263 and 22C3 assay positive cases corresponded to the CK5/6 SP subgroup. Besides, when classified into each subgroup analyzed each, the positive rate of all PD-L1 assays in each subgroup was significantly higher in the CK5/6 SP subgroup compared to other subgroups (Table 9 and Figure 8).

Table 9. Comparison of IHC-defined subgroups and PD-L1 positivity.

	CK5/6 SP	DP	CK20 SP	DN	Total
	n (%)	*n* (%)	*n* (%)	*n* (%)	
SP142					
Negative	38 (62.3%)	12 (92.3%)	68 (97.1%)	41 (91.1%)	159
Positive	23 (37.7%)	1 (7.7%)	2 (2.9%)	4 (8.9%)	30
SP263					
Negative	24 (39.3%)	10 (76.9%)	68 (97.1%)	39 (86.7%)	141
Positive	37 (60.7%)	3 (23.1%)	2 (2.9%)	6 (13.3%)	48
22C3					
Negative	31 (50.8%)	11 (84.6%)	68 (97.1%)	40 (88.9%)	150
Positive	30 (49.2%)	2(15.4%)	2 (2.9%)	5 (11.1%)	39

Abbreviations: CK5/6 SP, CK5/6 single-positive; CK20 SP, CK20 single-positive; DN, double-negative; DP, double-positive; IHC, immunohistochemistry.

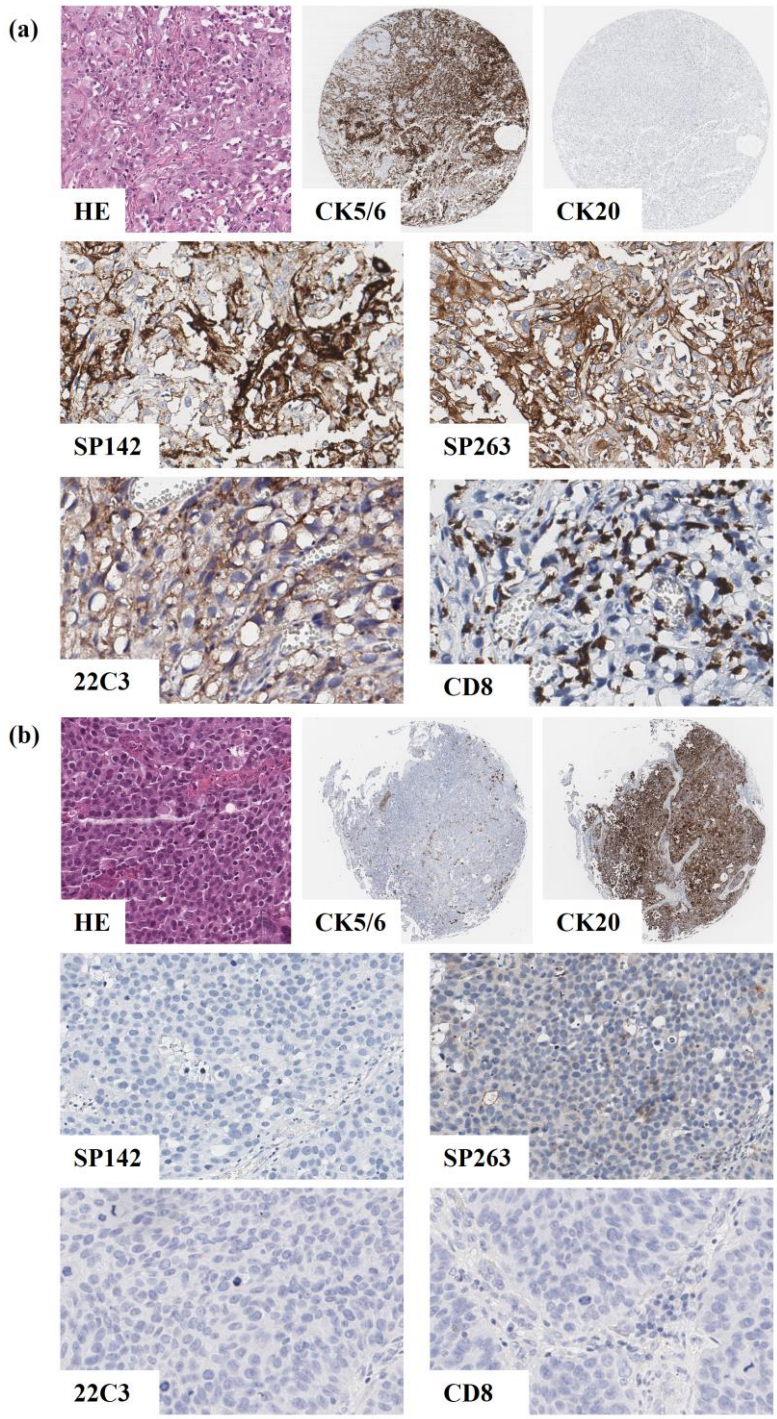

Figure 8. Representative images of CK5/6 SP and CK20 SP subgroup. (a) CK5/6 SP subgroup; PD-L1 assays are positive and CD8+ lymphocyte level is high. (b) CK20 SP subgroup; PD-L1 assays are negative and CD8+ lymphocyte level is low.

3.9. CD8+ lymphocyte numbers in IHC-based subgroups

The result of the CD8+ lymphocyte is summarized in Figure 9. Mean numbers of CD8+ lymphocyte was 58.3/HPF in the CK5/6 SP subgroup, 27.8/HPF in the DP subgroup, 17.0/HPF in the CK20 subgroup and 26.6/HPF in the DN subgroup. The CD8+ lymphocyte number was significantly different between the CK5/6 SP subgroup and other subgroups (all, p<0.01). With median score cut-off value applied, high CD8+ lymphocyte level was observed in 77.0% (47/66) in the CK5/6 SP subgroup, 46.2% (6/13) in the DP subgroup, 34.3% (24/70) in the CK20 SP subgroup and 48.9% (22/45) in the DN subgroup. And there was a significant correlation of high CD8+ lymphocyte level with PD-L1 SP 142, SP 263 and 22C3 assays positivity (all, p<0.001) (Table 10).

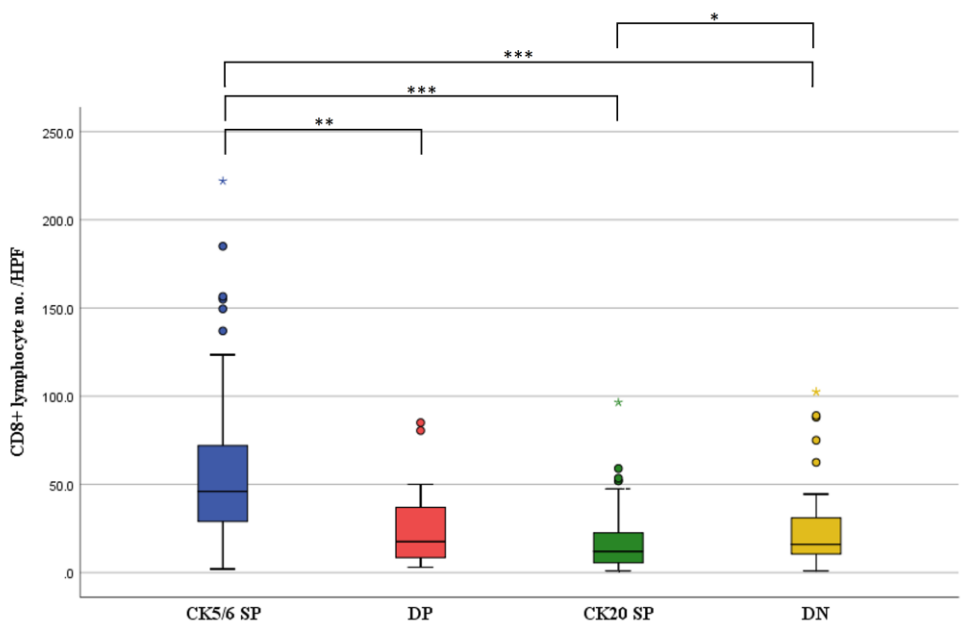

Figure 9. Comparison of CD8+ lymphocyte numbers between IHC-defined subgroups. (*, p=0.03; **, p=0.009; ***, p<0.001)

Table 10. Relationship between PD-L1 positivity and CD8+ lymphocyte.

		SP142			SP 263			22C3		
		Negative	Positive	*p*-Value	Negative	Positive	*p*-Value	Negative	Positive	*p*-Value
CD8	Low	90 (56.6%)	0 (0.0%)	<0.001	87 (61.7%)	3 (6.3%)	<0.001	88 (58.7%)	2 (5.1%)	<0.001
	High	69 (43.4%)	30 (100%)		54 (38.3%)	45 (93.8%)		62 (41.3%)	37 (94.9%)	

3.10. HER2 expression in IHC-based subgroups

The HER2 IHC results are summarized in Table 11. HER2 expression score was 3+ in 31 cases, 2+ in 21 case, 1+ in 50 cases and 0+ in 87 cases. The HER2 3+ results were significantly enriched with CK20 SP subgroup (21/31). Furthermore, it decreased in the DN (5/31), the CK5/6 SP (4/31), and the DP subgroup (1/31) in respective order (Figure 10). In the sequencing analysis using fresh-frozen tissue, *ERBB2* mRNA expression was the highest in the CK20 SP subgroup, which was followed by the DN, the DP, and the CK5/6 SP subgroup in respective order.

Table 11. Comparison of and HER2 expression between IHC-defined subgroups.

	CK5/6 SP	DP	CK20 SP	DN	Total
	n (%)	*n* (%)	*n* (%)	*n* (%)	*n*
HER2 negative (0, 1+)	57 (93.4%)	12 (92.3%)	32 (45.7%)	36 (80.0%)	137
HER2 equivocal (2+)	0 (0.0%)	0 (0.0%)	17 (24.3%)	4 (8.9%)	21
HER2 positive (3+)	4 (6.6%)	1 (7.7%)	21 (30.0%)	5 (11.1%)	31

Abbreviations: CK5/6 SP, CK5/6 single-positive; CK20 SP, CK20 single-positive; DN, double-negative; DP, double-positive; IHC, immunohistochemistry.

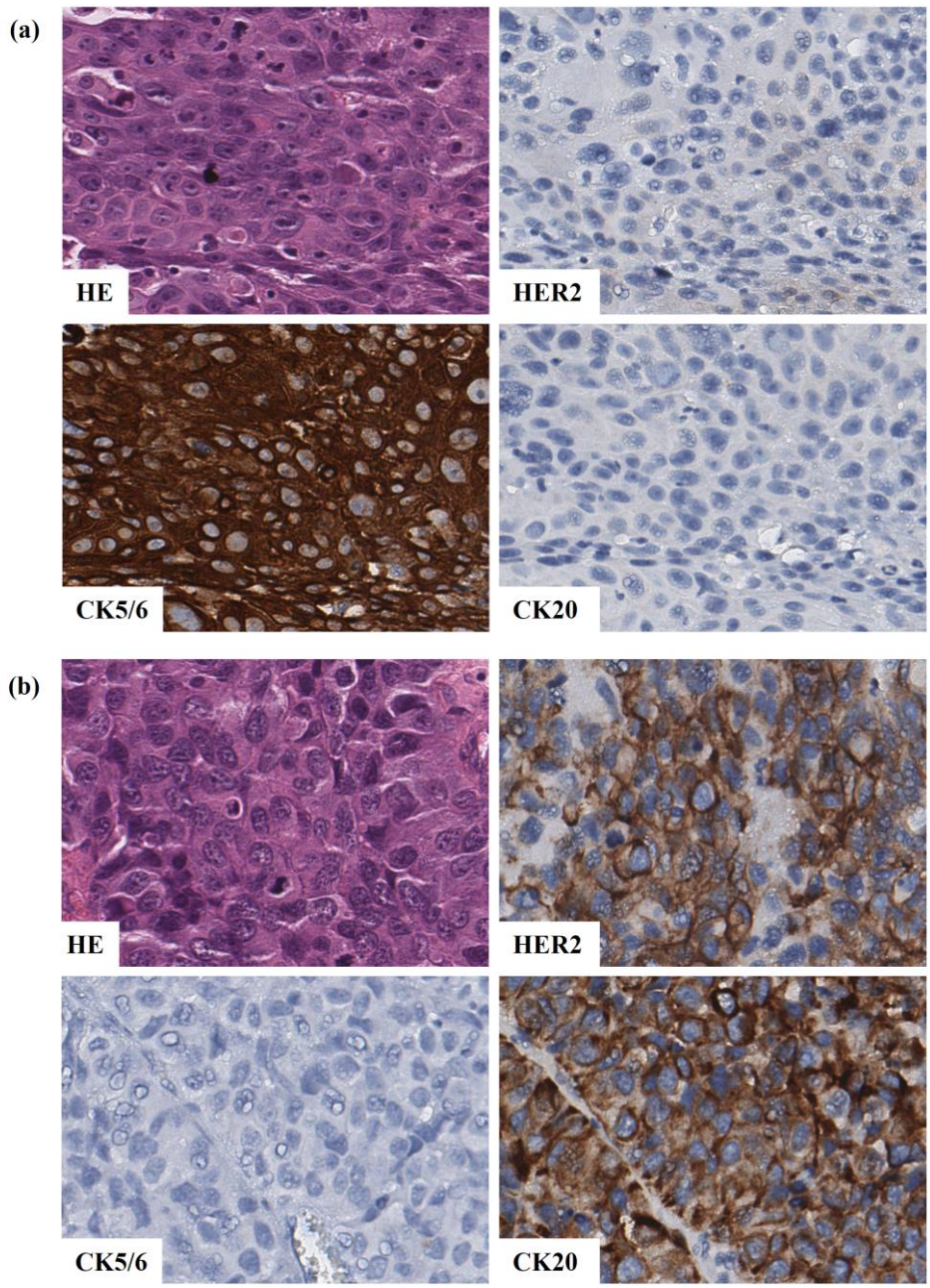

Figure 10. Representative images of HER2 expression. (a) CK5/6 SP subgroup; HER2 expression is negative. (b) CK20 SP subgroup; HER2 expression is positive.

3.11. Survival analysis of IHC-based subgroups

The follow-up period ranged from 1 to 277 months, the median follow-up period was 16 months, and the median survival period was 92 months. Of a total of 189 patients, clinical follow-up data for 185 patients were available. During the follow-up period, disease progression was found in 95 cases, and death occurred in 128 cases.

We performed the Kaplan–Meier survival analysis according to IHC-based classification. Of the four IHC-based subgroups, the CK5/6 SP subgroup had the worst PFS (p = 0.008). The Kaplan–Meier analysis also showed that the high expression of CK5/6 was associated with unfavorable PFS (p = 0.005) (Figure 11). In contrast, low expression of CK20 was associated with unfavorable PFS (p = 0.028). However, there was no significant difference in OS according to IHC-based classification (p = 0.709) or IHC expression (p = 0.840, CK5/6; p = 0.286, CK20).

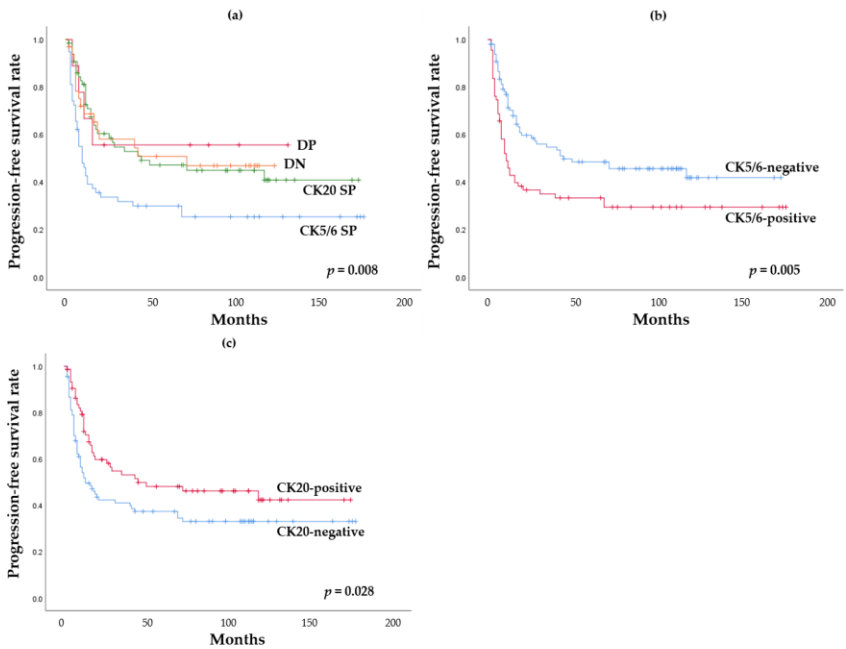

Figure 11. Progression free survival analysis: (a) impact of IHC-based classification; (b) impact of CK5/6 expression; (c) impact of CK20 expression.

4. Discussion

In recent years, research on molecular-based UB UC subtype classification has been actively underway. As gene expression profiles were reported to show different disease progressions, responses to chemotherapy and survival rates, the UB UC molecular subtype classification became a necessary step in UB UC diagnosis and treatment planning. In MIBC, the basal type is known to arise from basal and stem cells of normal urothelium, and the luminal type is known to arise from terminally differentiated superficial umbrella cells [31]. During urothelium differentiation, basal and intermediate cells express *KRT5* but do not express *KRT20*. Furthermore, terminal differentiation process is associated with suspension of *KRT5* expression and start of *KRT20* expression [32]. Additionally, as *KRT14* is also involved in this process, basal cells are known to show *KRT14+KRT5+KRT20-,* intermediate cells show *KRT14-KRT5+KRT20-,* and differentiated cells show *KRT14-KRT5-KRT20+* [33]. In MIBC, the basal subtype shows high expression of *KRT5, KRT6, KRT14, CD44* and *CDH3*, shows chemo-sensitive properties, is intrinsically aggressive, and is associated with poor prognosis. The luminal subtype shows high expression of *UPK, KRT20, FOXA1,* and *GATA3*, shows chemo-resistant properties, and seems to be less aggressive [31]. In addition to mRNA levels, IHC protein level markers include CK5/6 and CK14 for the basal subtype and CK20, GATA3, and Uroplakin2 for the luminal subtype. Furthermore, one study indicated that expression of CK5/6 and CK20 was inversely related in MIBC [3]. Based on these results, in a practical context, affordable IHC antibodies, CK5/6 and CK20, were selected as surrogate markers for IHC-based subgroup classification.

Previous studies utilized NGS analysis to assess gene expression patterns and reported differences in CK expression patterns between molecular subtypes. In this study, we took a different approach in case selection. Cases of the CK5/6 SP, CK20

SP, DP and DN subgroups were selected based on CK IHC results, and gene expression profiles were evaluated with these cases. Furthermore, based on IHC, CK5/6 and CK20 protein expression areas were accurately evaluated before tissue collection, which led to more precise tumor tissue collection.

MIBC cases with sufficient fresh-frozen tissues were included, which resulted in 30 samples classified to four subgroups based on CK5/6 and CK20 IHC results. Nine cases in the DP subgroup and five cases in the DN subgroup among 30 cases may indicate a relatively high proportion of the DP and DN subgroups in UB UC molecular subtype classification. The DP and DN subgroup cases may be in a stage of transition between molecular subtypes or they may be subtypes completely independent from the CK5/6 SP and CK20 SP subgroups. However, research regarding this aspect of subtype classification has not been presented to date. Compared to the CK5/6 SP and CK20 SP subgroups, the DP subgroup showed a relatively high expression of basal- and luminal-type markers, which gave us the impression of a mixed phenotype. This subgroup showed the strongest immune signature genes expression. However, in GO, IPA, and GSEA functional analysis, the DP subgroup did not show a significant difference from the CK5/6 SP subgroup. Based on these results, the DP subgroup was expected to be close to the CK5/6 SP subgroup in tumor characteristic aspects. The DN subgroup, in every comparison with the three other subgroups, showed the highest number on GO and KEGG pathways with significant differences. The DN subgroup also showed mostly low gene expression on biological signature gene cluster expression analysis. In GO, IPA, and GSEA functional analysis, the DN subgroup showed no significant difference from the CK20 SP subgroup, except for “activation of cells associated molecules”, in the IPA result. The DN subgroup is the most similar to the CK20 SP subgroup among the three other subgroups, but we think it is a unique subtype that shows differences in gene expression from the other subgroups.

Expression of p63-associated genes was high in the CK5/6 SP and DP subgroups. *TP63*, which is a transcription factor associated with basal/stem cells in the urothelium, is known to be activated in the basal-type MIBC and to regulate basal gene expression signature [3]. In line with previous studies, which reported that p63-associated genes were enriched in the basal-type MIBC, CK5/6 SP and DP subgroups showed high expression of p63-associated genes.

In comparison between subgroups, expression of TP53-like signature genes was the lowest in the DN subgroup and varied among cases. Six cases, which showed diffusely strong positive results on IHC, showed high expression of TP53-associated gene mRNA. Association between *TP53* mRNA expression and p53 IHC protein expression showed a positive correlation.

Expression of immune response-associated genes was high in the DP subgroup, and the CK5/6 SP, DN, and CK20 SP subgroups followed in respective order. Dividing the genes into two groups based on CK5/6 IHC results, immune response GO term associated DEGs were more enriched and associated genes were more upregulated in CK5/6-positive group (DP and CK5/6 SP subgroups) than in CK5/6-negative group (DN and CK20 SP subgroups). Additionally, on IPA analysis, immune activation was more upregulated in DP and CK5/6 SP subgroups than in the other subgroups. In a previous study in our group, it was found that PD-L1 expression was enriched in the BASQ subtype positive for CK5/6 and CK14 on IHC [34]. These results correlate with previous studies, which reported high immune gene signature expression in the basal subtype [8, 35].

Expression of EMT marker was enriched in the DP and CK5/6 SP subgroups. The EMT is the process of epithelial or endothelial cells acquiring mesenchymal phenotypes, and is associated with tumor progression and metastasis process [36-39]. Furthermore, some studies reported that, in various cancers, EMT showed a strong correlation with immune activation, and had high expression

of *programmed cell death-1 (PD-1), PD-L1, CTLA4, OX40L* and *PD-L2*. In these studies, activation of the immune cell signaling pathway was observed in the EMT setting, which was interpreted as an indication that the EMT may facilitate a change of the tumor microenvironment [40, 41]. Additionally, Chen et al. suggested that microRNA-200 (miR-200) formed a negative feedback loop with ZEB1, an EMT activator, suppressed the EMT, and suppressed PD-L1 expression. These authors demonstrated that the EMT is linked to the immunosuppression through the miR-200/ZEB1 axis [42, 43]. The miR-200 family is known to be enriched in the luminal type, which also correlates well with the results of this study, as CK20 SP and DN subgroups showed low EMT and immune response-associated gene expression [3].

Expression of cell adhesion markers showed low expression of tight junction-related genes *TPJ2* and *CLDN4* and high expression of desmosome-related genes *DSC3* and *PKP1*, gap junction-related genes *GJB3* and *GLB4*, and epithelial integrin genes *ITGA6* and *ITGB4* in the CK5/6 SP subgroup. These results imply that the CK5/6 SP subgroup shows increased expression of cell adhesion, especially basolateral cell adhesion-related genes. This result is in keeping with previous studies, which reported high cell adhesion gene expression signature in the mRNA-based basal subtype, including urobasal B and SCC-like subtype [24].

Expression of the MAPK and TNF signaling pathways was enriched in the DP and CK5/6 SP subgroups. Most of the DEGs associated with these signaling pathway were upregulated in the DP and CK5/6 SP subgroups.

On GSEA analysis, the IL6-JAK-STAT3 signaling pathway and TNF-α signaling via NF-κB signaling pathway were significantly enriched in the DP and CK5/6 SP subgroups. In contrast, the DN subgroup was found to be less sensitive to this pathway. The IL6-JAK-STAT3 signaling pathway is upregulated in various types of cancer and its hyperactivation is associated with adverse clinical outcome [44-46]. Furthermore, the TNF-α/NF-

κB signaling pathway is known to be involved in the tumor invasion and metastasis [47, 48]. Considering the GSEA results, the CK5/6-positive group (CK5/6 SP and DP subgroups) is a more aggressive subtype than the CK5/6-negative or at least the DN subgroup.

On IPA analysis, compared to the other subgroups, the DN subgroup showed downregulated cell movement, cell migration, and cell activation. Such cellular functions, which are associated with cell motility, are closely related to cancer invasion and cancer metastasis [49-52]. Based on IPA analysis we can expect the DN subgroup to have a less aggressive behavior than the three other subgroups.

In phase II clinical trial of CheckMate 275 different nivolumab immunotherapy response was reported among molecular subtypes in patients with metastatic UC, of which it was the highest in TCGA cluster III [15]. Additionally, in a clinical trial using the SP142 assay, mRNA based TCGA clusters III and IV, which correspond to the basal type, showed highly enriched PD-L1 IC and TC expression, and TCGA cluster II, which corresponds to the luminal type, showed a significantly higher response to atezolizumab, a humanized monoclonal anti PD-L1 antibody, than clusters III and IV [13]. Our present results showing high PD-L1 expression in CK5/6 SP subgroup are in line with previous research.

In a previous study, Hodgson et al. suggested that MIBC could be classified into luminal and basal subtypes using CK5/6 and GATA3 IHC, and each subtype was analyzed for its PD-L1 SP263 expression and tumor infiltrating lymphocytes. The results showed that PD-L1 positivity was more common in the basal subtype, and that CD8+ T cells and PD-L1 expression were also significantly associated with the basal subtype [16].

In this study, we additionally analyzed the PD-L1 expression status using SP142, SP263 and 22C3 in MIBC immunohistochemically defined molecular subtypes. We evaluated PD-L1 expression using three PD-L1 assays (SP142, SP263 and 22C3), and the overall concordance rate of PD-L1 positive status

was substantial and almost perfect, in line with previous studies [53]. We demonstrated that a high PD-L1 positive rate was significantly associated with the CK5/6 SP subgroup. Furthermore, we demonstrated that a high PD-L1 positive rate was significantly associated with positive CK5/6, CK14 and CD44 expression and negative CK20, GATA3 and FOXA1 expression.

T lymphocytes eliminate tumor cells through immune surveillance using T cell receptor and major histocompatibility complex interaction. The interaction of PD-1 expressed in T lymphocyte with PD-L1 expressed in tumor cell leads to obstacles in immune regulation described above. PD-1/PD-L1 pathway is used by tumor cells as a method of immune evasion. But, PD-L1 expression on clinical prognosis is poorly defined in UC. Some studies have suggested that PD-L1 overexpression was correlated with poor prognosis in bladder cancer [54-56]. On the other hand, some studies reported that PD-L1 expression was no correlation with clinical outcome in UC [57, 58].

The role of PD-L1 expression as a predictive biomarker also has many points to consider. There are clinical trial results that show that PD-L1 expression and response rate of PD-1/PD-L1 blockades are insufficiently related [59]. However, currently, it is clear that PD-L1 expression is a companion or complementary diagnostic test of PD-1/PD-L1 blockades and a potential predictive biomarker. And it is generally accepted that PD-1/PD-L1 blockades has been known to have a higher efficacy in patients whose immune cells express PD-L1. The positive PD-L1 expression rate in IHC-based subgroups can help to determine a treatment strategy in MIBC. To the best of our knowledge, our study is the first to analyze the association of IHC-defined subgroups with three PD-L1 assays (SP142, SP263 and 22C3) in MIBC. The significant difference of positive rate of PD-L1 assays according to IHC-based classification suggests that IHC-based classification may be important to apply the PD-1/PD-L1 blockade treatment in patients with MIBC.

mRNA sequencing analysis was carried out after selecting areas composed of mainly tumor cells, excluding any peri-tumoral stroma including inflammatory cells. In contrast, PD-L1 and CD8 IHC analysis results reflected tumor cells as well as peri-tumoral inflammatory cells. In PD-L1 analysis, SP142 assay only reflected immune cells, and SP263 and 22C3 assay reflected tumor and immune cells. In CD8 IHC analysis, lymphocytes showing CD8 membranous staining were counted.

As described above, mRNA expression only reflects tumor cells and IHC protein expression either reflects only immune cells, or reflects tumor and immune cells together, which can lead to a discrepancy between their results. Especially, the CK5/6 SP subgroup showed higher PD-L1 positivity and CD8+ lymphocyte numbers than mRNA expression. The CK5/6 SP subgroup, compared to other subgroups, showed higher EMT-associated gene expression, upregulation of signaling pathways related to tumor aggressiveness, and poorer PFS outcome. In our opinion, CK5/6 SP is accompanied by tumor microenvironment changes, which can lead to a stronger immune response, resulting in high PD-L1 and CD8 IHC expression.

We evaluated HER2 protein expression in 189 cases of MIBC. HER2 is a well-established therapeutic target in some forms of cancer characterized by HER2 protein overexpression or gene amplification [60, 61]. MIBC has the third highest incidence of *ERBB2* amplification after breast and gastric cancer [4], thus, targeted therapy against HER2 has been attempted in patients with UC showing HER2 gene amplification [62, 63]. Our study revealed that the CK20 SP subgroup frequently showed HER2 protein expression. These results are in line with previous studies, which reported that HER2 alteration was high in the luminal TCGA clusters, and that *ERBB2* amplification and HER2 protein expression were significantly higher in the luminal TCGA clusters compared to basal TCGA clusters [23]. The results of our study suggest that classification of MIBC according to the IHC could be suggested as a

potential marker for HER2-targeted therapy.

Different molecular subtypes were reported to have different prognoses and chemotherapy sensitivity in MIBC. In addition, we also found that the IHC-based classification has prognostic value. Compared with the CK5/6-negative group (CK20 SP and DN subgroups), the CK5/6-positive group (CK5/6 SP and DP subgroups), which implies the high EMT, IL6-JAK-STAT3 signaling pathway, TNF-α/NF-κB signaling pathway and immune gene expression signature, show adverse disease progression outcome, and this result is in keeping with the findings of previous studies [3, 5]. It is assumed that the effective immune escape process that arises by expression of PD-L1 may be related to disease progression. Although the DP subgroup showed no difference in disease progression rate from other CK20 SP and DN subgroups, this consequence is considered because there were very few cases of the DP subgroup in this study population. In contrast to the PFS, there was no significant difference in OS rate between IHC-defined subgroups. The difference in PFS for each subgroup but no difference in OS can be interpreted as meaning that the post-progression period is considerably long. We think this is related to the fact that most of the subjects of this study consist of pathologic stage T2 cases. Since it was composed of cases with a good overall prognosis, there was no significant difference in the OS analysis for each subgroup.

In the personalized precision medicine era, subgrouping of patients based on molecular characteristics has considerable influence on selecting therapeutic regimens and forecasting therapeutic responses and prognoses. In addition, mRNA sequencing analysis is a good method to examine phenotype characteristics of a tumor, however, in this study we utilized an IHC-based classification that is simpler and more affordable. We examined the molecular characteristics of subgroups based on IHC classification. In summary, we found that the CK5/6-positive group showed a high gene expression signature related to aggressive

behavior, high positivity of PD-L1 assays and showed worse clinical outcomes.

Bibliography

1. Bray F, Ferlay J, Soerjomataram I et al. Global cancer statistics 2018: GLOBOCAN estimates of incidence and mortality worldwide for 36 cancers in 185 countries. CA Cancer J Clin 2018; 68: 394-424.

2. Van Batavia J, Yamany T, Molotkov A et al. Bladder cancers arise from distinct urothelial sub-populations. Nat Cell Biol 2014; 16: 982-991, 981-985.

3. Choi W, Porten S, Kim S et al. Identification of distinct basal and luminal subtypes of muscle-invasive bladder cancer with different sensitivities to frontline chemotherapy. Cancer Cell 2014; 25: 152-165.

4. Cancer Genome Atlas Research N. Comprehensive molecular characterization of urothelial bladder carcinoma. Nature 2014; 507: 315-322.

5. Damrauer JS, Hoadley KA, Chism DD et al. Intrinsic subtypes of high-grade bladder cancer reflect the hallmarks of breast cancer biology. Proc Natl Acad Sci U S A 2014; 111: 3110-3115.

6. Lerner SP, McConkey DJ, Hoadley KA et al. Bladder Cancer Molecular Taxonomy: Summary from a Consensus Meeting. Bladder Cancer 2016; 2: 37-47.

7. Sjodahl G, Eriksson P, Liedberg F, Hoglund M. Molecular classification of urothelial carcinoma: global mRNA classification versus tumour-cell phenotype classification. J Pathol 2017; 242: 113-125.

8. Robertson AG, Kim J, Al-Ahmadie H et al. Comprehensive Molecular Characterization of Muscle-Invasive Bladder Cancer. Cell 2017; 171: 540-556 e525.

9. McConkey DJ, Choi W, Dinney CP. Genetic subtypes of invasive bladder cancer. Curr Opin Urol 2015; 25: 449-458.

10. McConkey DJ, Choi W, Ochoa A et al. Therapeutic opportunities in the intrinsic subtypes of muscle-invasive bladder cancer. Hematol Oncol Clin North Am 2015; 29: 377-394, x-xi.

11. Seiler R, Ashab HAD, Erho N et al. Impact of Molecular Subtypes in Muscle-invasive Bladder Cancer on Predicting Response and Survival after Neoadjuvant Chemotherapy. Eur Urol 2017; 72: 544-554.
12. Kim J, Kwiatkowski D, McConkey DJ et al. The Cancer Genome Atlas Expression Subtypes Stratify Response to Checkpoint Inhibition in Advanced Urothelial Cancer and Identify a Subset of Patients with High Survival Probability. Eur Urol 2019; 75: 961-964.
13. Rosenberg JE, Hoffman-Censits J, Powles T et al. Atezolizumab in patients with locally advanced and metastatic urothelial carcinoma who have progressed following treatment with platinum-based chemotherapy: a single-arm, multicentre, phase 2 trial. Lancet 2016; 387: 1909-1920.
14. Tan TZ, Rouanne M, Tan KT et al. Molecular Subtypes of Urothelial Bladder Cancer: Results from a Meta-cohort Analysis of 2411 Tumors. Eur Urol 2019; 75: 423-432.
15. Sharma P, Retz M, Siefker-Radtke A et al. Nivolumab in metastatic urothelial carcinoma after platinum therapy (CheckMate 275): a multicentre, single-arm, phase 2 trial. Lancet Oncol 2017; 18: 312-322.
16. Hodgson A, Liu SK, Vesprini D et al. Basal-subtype bladder tumours show a 'hot' immunophenotype. Histopathology 2018; 73: 748-757.
17. Sasaki Y, Sasaki T, Kawai T et al. HER2 protein overexpression and gene amplification in upper urinary tract urothelial carcinoma-an analysis of 171 patients. Int J Clin Exp Pathol 2014; 7: 699-708.
18. Kruger S, Weitsch G, Buttner H et al. HER2 overexpression in muscle-invasive urothelial carcinoma of the bladder: prognostic implications. Int J Cancer 2002; 102: 514-518.
19. Gunia S, Koch S, Hakenberg OW et al. Different HER2 protein expression profiles aid in the histologic differential diagnosis between urothelial carcinoma in situ (CIS) and non-CIS conditions (dysplasia and reactive atypia) of the urinary bladder mucosa. Am J

Clin Pathol 2011; 136: 881-888.
20. Kolla SB, Seth A, Singh MK et al. Prognostic significance of Her2/neu overexpression in patients with muscle invasive urinary bladder cancer treated with radical cystectomy. Int Urol Nephrol 2008; 40: 321-327.
21. Lae M, Couturier J, Oudard S et al. Assessing HER2 gene amplification as a potential target for therapy in invasive urothelial bladder cancer with a standardized methodology: results in 1005 patients. Ann Oncol 2010; 21: 815-819.
22. Hansel DE, Swain E, Dreicer R, Tubbs RR. HER2 overexpression and amplification in urothelial carcinoma of the bladder is associated with MYC coamplification in a subset of cases. Am J Clin Pathol 2008; 130: 274-281.
23. Kiss B, Wyatt AW, Douglas J et al. Her2 alterations in muscle-invasive bladder cancer: Patient selection beyond protein expression for targeted therapy. Sci Rep 2017; 7: 42713.
24. Sjodahl G, Lauss M, Lovgren K et al. A molecular taxonomy for urothelial carcinoma. Clin Cancer Res 2012; 18: 3377-3386.
25. Sjodahl G, Lovgren K, Lauss M et al. Toward a molecular pathologic classification of urothelial carcinoma. Am J Pathol 2013; 183: 681-691.
26. Dadhania V, Zhang M, Zhang L et al. Meta-Analysis of the Luminal and Basal Subtypes of Bladder Cancer and the Identification of Signature Immunohistochemical Markers for Clinical Use. EBioMedicine 2016; 12: 105-117.
27. Wolff AC, Hammond MEH, Allison KH et al. Human Epidermal Growth Factor Receptor 2 Testing in Breast Cancer: American Society of Clinical Oncology/College of American Pathologists Clinical Practice Guideline Focused Update. Arch Pathol Lab Med 2018; 142: 1364-1382.
28. Kundel HL, Polansky M. Measurement of observer agreement. Radiology 2003; 228: 303-308.
29. Amin MB ES, Greene F, Byrd DR, Brookland RK, Washington MK, Gershenwald JE, Compton CC, Hess KR, et al. (Eds.). AJCC

Cancer Staging Manual (8th edition). In. Springer International Publishing: American Joint Commission on Cancer 2017; 739-748.
30. Eble JN SG, Epstein JI, Sesterhenn IA. World Health Organization classification of tumors: pathology and genetics of tumours of the urinary system and male genital organs. Lyon: IARC Press, 2016.
31. Choi W, Czerniak B, Ochoa A et al. Intrinsic basal and luminal subtypes of muscle-invasive bladder cancer. Nat Rev Urol 2014; 11: 400-410.
32. de la Rosette J, Smedts F, Schoots C et al. Changing patterns of keratin expression could be associated with functional maturation of the developing human bladder. Journal of Urology 2002; 168: 709-717.
33. Volkmer JP, Sahoo D, Chin RK et al. Three differentiation states risk-stratify bladder cancer into distinct subtypes. Proc Natl Acad Sci U S A 2012; 109: 2078-2083.
34. Kim B, Lee C, Kim YA, Moon KC. PD-L1 Expression in Muscle-Invasive Urinary Bladder Urothelial Carcinoma According to Basal/Squamous-Like Phenotype. Front Oncol 2020; 10: 527385.
35. Kardos J, Chai S, Mose LE et al. Claudin-low bladder tumors are immune infiltrated and actively immune suppressed. JCI Insight 2016; 1: e85902.
36. Zeisberg M, Neilson EG. Biomarkers for epithelial-mesenchymal transitions. J Clin Invest 2009; 119: 1429-1437.
37. Hugo H, Ackland ML, Blick T et al. Epithelial--mesenchymal and mesenchymal--epithelial transitions in carcinoma progression. J Cell Physiol 2007; 213: 374-383.
38. Thiery JP, Acloque H, Huang RY, Nieto MA. Epithelial-mesenchymal transitions in development and disease. Cell 2009; 139: 871-890.
39. Huber MA, Kraut N, Beug H. Molecular requirements for epithelial-mesenchymal transition during tumor progression. Curr Opin Cell Biol 2005; 17: 548-558.
40. Byers LA, Diao L, Wang J et al. An epithelial-mesenchymal

transition gene signature predicts resistance to EGFR and PI3K inhibitors and identifies Axl as a therapeutic target for overcoming EGFR inhibitor resistance. Clin Cancer Res 2013; 19: 279-290.
41. Mak MP, Tong P, Diao L et al. A Patient-Derived, Pan-Cancer EMT Signature Identifies Global Molecular Alterations and Immune Target Enrichment Following Epithelial-to-Mesenchymal Transition. Clin Cancer Res 2016; 22: 609-620.
42. Chen L, Gibbons DL, Goswami S et al. Metastasis is regulated via microRNA-200/ZEB1 axis control of tumour cell PD-L1 expression and intratumoral immunosuppression. Nat Commun 2014; 5: 5241.
43. Gregory PA, Bert AG, Paterson EL et al. The miR-200 family and miR-205 regulate epithelial to mesenchymal transition by targeting ZEB1 and SIP1. Nat Cell Biol 2008; 10: 593-601.
44. Kusaba T, Nakayama T, Yamazumi K et al. Activation of STAT3 is a marker of poor prognosis in human colorectal cancer. Oncol Rep 2006; 15: 1445-1451.
45. Macha MA, Matta A, Kaur J et al. Prognostic significance of nuclear pSTAT3 in oral cancer. Head Neck 2011; 33: 482-489.
46. Johnson DE, O'Keefe RA, Grandis JR. Targeting the IL-6/JAK/STAT3 signalling axis in cancer. Nat Rev Clin Oncol 2018; 15: 234-248.
47. Wu Y, Zhou BP. TNF-alpha/NF-kappaB/Snail pathway in cancer cell migration and invasion. Br J Cancer 2010; 102: 639-644.
48. Xia Y, Shen S, Verma IM. NF-kappaB, an active player in human cancers. Cancer Immunol Res 2014; 2: 823-830.
49. Stuelten CH, Parent CA, Montell DJ. Cell motility in cancer invasion and metastasis: insights from simple model organisms. Nat Rev Cancer 2018; 18: 296-312.
50. Yamaguchi H, Condeelis J. Regulation of the actin cytoskeleton in cancer cell migration and invasion. Biochim Biophys Acta 2007; 1773: 642-652.
51. Yilmaz M, Christofori G. Mechanisms of motility in metastasizing

cells. Mol Cancer Res 2010; 8: 629-642.
52. Clark AG, Vignjevic DM. Modes of cancer cell invasion and the role of the microenvironment. Curr Opin Cell Biol 2015; 36: 13-22.
53. Rijnders M, van der Veldt AAM, Zuiverloon TCM et al. PD-L1 Antibody Comparison in Urothelial Carcinoma. Eur Urol 2019; 75: 538-540.
54. Ding X, Chen Q, Yang Z et al. Clinicopathological and prognostic value of PD-L1 in urothelial carcinoma: a meta-analysis. Cancer Manag Res 2019; 11: 4171-4184.
55. Zhu L, Sun J, Wang L et al. Prognostic and Clinicopathological Significance of PD-L1 in Patients With Bladder Cancer: A Meta-Analysis. Front Pharmacol 2019; 10: 962.
56. Wang B, Pan W, Yang M et al. Programmed death ligand-1 is associated with tumor infiltrating lymphocytes and poorer survival in urothelial cell carcinoma of the bladder. Cancer Sci 2019; 110: 489-498.
57. Faraj SF, Munari E, Guner G et al. Assessment of tumoral PD-L1 expression and intratumoral CD8+ T cells in urothelial carcinoma. Urology 2015; 85: 703 e701-706.
58. Bellmunt J, Mullane SA, Werner L et al. Association of PD-L1 expression on tumor-infiltrating mononuclear cells and overall survival in patients with urothelial carcinoma. Ann Oncol 2015; 26: 812-817.
59. Aggen DH, Drake CG. Biomarkers for immunotherapy in bladder cancer: a moving target. J Immunother Cancer 2017; 5: 94.
60. Tinoco G, Warsch S, Gluck S et al. Treating breast cancer in the 21st century: emerging biological therapies. J Cancer 2013; 4: 117-132.
61. Smyth EC, Cunningham D. Targeted therapy for gastric cancer. Curr Treat Options Oncol 2012; 13: 377-389.
62. Ikeda S, Hansel DE, Kurzrock R. Beyond conventional chemotherapy: Emerging molecular targeted and immunotherapy strategies in urothelial carcinoma. Cancer Treat Rev 2015; 41: 699-706.

63. Hussain MH, MacVicar GR, Petrylak DP et al. Trastuzumab, paclitaxel, carboplatin, and gemcitabine in advanced human epidermal growth factor receptor-2/neu-positive urothelial carcinoma: results of a multicenter phase II National Cancer Institute trial. J Clin Oncol 2007; 25: 2218-2224.

국문초록

면역조직화학염색을 통해 분류한 근육침윤성 방광 요로상피암 소집단간의 분자유전학적 발현 비교 분석

김보현
서울대학교 대학원
의학과 병리학 전공

서론: 다양한 mRNA기반 요로상피암 분류법들이 보고되고 있다. 각 분자아형마다 치료반응, 예후적 특징이 이질적이라고 알려져 있다.

방법: 본 연구에서는 CK5/6, CK20에 대한 면역조직화학염색 결과에 따라 근육침윤성 방광 요로상피암을 구분하였다. CK5/6 단일 양성 소그룹, CK20 단일 양성 소그룹, 이중 양성 소그룹, 이중 음성 소그룹으로 분류하였고 각 소그룹별로 구분하여 유전자 발현을 확인하였다. 그리고 189명의 근육침윤성 방광 요로상피암 환자 조직 마이크로어레이에 CK5/6, CK20, CK14, CD44, GATA3, FOXA1 그리고 PD-L1 (SP142, SP263 and 22C3) 면역조직화학염색을 시행하였다.

결과: 차별 발현유전자를 이용한 유전자 온톨로지 분석과 기능분석 결과, 세포 이동, 면역반응 활성화, IL6-JAK-STAT3 신호전달, NF- κB를 통한 tumor necrosis factor- α 신호전달 관여 유전자들은 CK5/6 단일 양성 및 이중 양성 소그룹에 더 관여되는 것으로 나타났다. 그리고 다른 소그룹들과 비교했을 때, 이중 음성 소그룹은 세포운동, 세포이동과 세포 활성화 관련 유전자가 저해되어 있었다. PD-L1 발현을 다음 세 가

지 항체를 (SP142, SP263 그리고 22C3) 이용하여 분석하였다. PD-L1 세 항체 모두 높은 양성율은 CK5/6 양성, CK14 양성, CD44 양성, CK20 음성, GATA3 음성 그리고 FOXA1 음성소견과 밀접한 연관성을 보였다. 면역조직화학염색 기반 분류 소그룹별로 비교했을 때, CK5/6 단일 양성 소그룹이 가장 높은 PD-L1 양성율을 보였다. 그리고 카플란-마이어 생존분석을 통해 CK5/6 단일 양성 소그룹이 더 짧은 무진행 생존기간을(p = 0.008) 가진다는 사실을 밝혔다.

결론: 본 연구를 통해 면역조직화학염색 기반 분류가 근육침윤성 방광 요로상피암 환자에서 PD-1/PD-L1 억제 면역항암제 적용하는 데 있어 중요한 역할을 할 가능성을 제시하였다. 그리고 CK5/6 양성 그룹이 종양 악성화와 관련된 유전자를 높게 발현하며, 불량한 예후를 보이는 사실을 밝혔다.

주요어: 근육침윤성 방광 요로상피암; 분자유전학적 분류; 면역조직화학염색; cytokeratin 5/6; cytokeratin 20; PD-L1

학번: 2015-31203